Wiley
International Journal of Energy Research
Volume 2024, Article ID 1847943, 21 pages
https://doi.org/10.1155/2024/1847943

WILEY

Review Article

Eletrospinning: Improving the Performance of 1-D Nanofibers Used in Anodes, Cathodes, and Separators in Lithium-Ion Batteries

JinUk Yoo, Dong Hyun Kim, and Sung Gyu Pyo

School of Integrative Engineering, Chung-Ang University, 84, Heukseok-ro, Dongjak-gu, Seoul 06974, Republic of Korea

Correspondence should be addressed to Sung Gyu Pyo; sgpyo@cau.ac.kr

Received 23 April 2024; Accepted 9 July 2024

Academic Editor: Suresh Kannan Balasingam

Electrospinning enables the rapid and facile production of nanofibers with desired structures and morphologies at room temperature and ambient pressure. These nanofibers are suitable cathode, anode, and separator materials for Li-ion batteries (LIBs) because of their one-dimensional(1-D) structures and mechanical strength as well as their ability to enable rapid Li-ion transport through short diffusion pathways. The use of electrospun nanofibers in LIBs can lead to better battery rechargeability, lifespan, and performance than those of existing LIBs. In this review article, we first discuss the problems associated with the cathode, anode, and separator materials currently used in LIBs. Next, we describe the improvements achieved by incorporating electrospun nanofibers as cathode, anode, and separator materials in LIBs. We believe that electrospun nanofibers can promote the advancement of LIB technology to realize very-high-energy-density energy storage systems.

1. Introduction

The continuous development of the global economy necessitates the replacement of the traditional nonrenewable energy sources of coal and oil with renewable energy sources. In particular, power generation from solar and wind resources has limitations, as energy can only be produced on sunny or windy days, that is, power generation depends on the weather. Moreover, as the number of mobile devices (smartphones, tablets, etc.) and electric vehicles increases, the demand for electric energy is growing exponentially, and better energy storage systems (ESS) are essential [1, 2, 3].

Rechargeable batteries, which are promising, high-energy-density ESSs, can help reduce our dependence on fossil fuels. Some examples of rechargeable batteries are Ni–Cd, Ni–MH, lithium-ion batteries (LIBs), lead–acid, and sodium–sulfur batteries. Among them, LIBs have advantages such as a long lifespan, high energy density, fast charging speed, weight reduction, reduced capacity charge, and portability. They are also environmental friendly because they do not contain toxic substances such as Pb oxide. The advancement of LIB technology enabled the development of lightweight smartphones, laptops, and tablets as well as electrical vehicles. However, Li, which exists in very small amounts on earth, is becoming expensive due to the increasing demand. Hence, large-scale applications of Li resources may not be feasible [3, 4]. Therefore, new LIBs that require smaller amounts of Li and enhanced performances must be developed. One strategy is to use nanosized Li particles in powder form. Nanoscale materials and composites have a facile charge-conduction mechanism, excellent textural properties, better interfaces, and chemical reaction rates. Additionally, the high surface-to-volume ratio and excellent mechanical strength of the nanostructure enable shorter ionic paths, increasing electrical conductivity [5]. Notably, researchers have theoretically proven that the use of nanoscale Li in LIBs results in higher energy density, a faster charge/discharge rate, and excellent cycling stability. However, Li metal particles have a long diffusion path and low electrode kinetic reaction rates, resulting in poor LIB performance. Therefore, using nanofibers, which have a one-dimensional (1-D) structure with a high area/mass ratio, a shorter diffusion path, and faster intercalation kinetics than the powder material, as an electrode material can reduce the amount of Li used in LIBs, thereby reducing the cost of

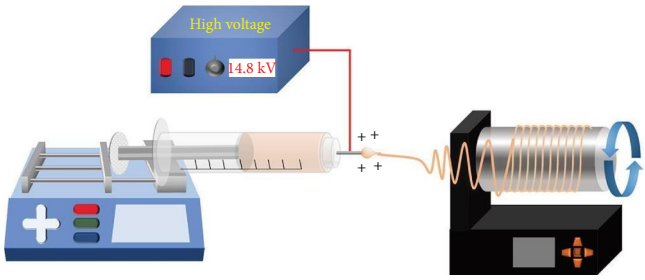

Figure 1: Schematic diagram of the electrospinning method. Equipment: high voltage supply, syringe pump, rotating collector, plastic syringe, and metallic needle tip.

LIBs and enhancing their performance [1, 5]. 1-D nanofibers have advantages such as high surface area, excellent mechanical strength, a high surface-to-volume ratio, and flexibility. These nanofibers maintain good contact with the current collector and enable facile Li diffusion during high-current operation. Electrospinning is a simple and quick method to fabricate 1-D nanofibers at room temperature and pressure [6, 7]. It is widely used to fabricate 2D or 3D mechanically stable, flexible, and conductive nanofiber electrodes for LIBs [8, 9].

2. Electrospinning

2.1. Advantages of Electrospinning. To fabricate 1-D nanofibers, the following equipment is required: a polymer solution placed in a syringe with a metallic nozzle, a high voltage supply for the formation of an electric field, and a metal collector that collects the fibers. Figure 1 illustrates the electrospinning process using a rotating type collector. Electrospinning can be used to fabricate not only single fibers but also core–shell structures using a coaxial nozzle, hollow structures by removing the core from the core–shell, and porous structures by adjusting the electrospinning parameters. Therefore, the surface area of the fibers can be rapidly and significantly increased by simply adjusting the parameters according to their use.

During the procedure, an electric field is generated by applying the high voltage between the syringe containing the polymer solution and the metallic collector. This causes the polymer solution at the needle tip to elongate and form a Taylor cone. When the voltage reaches a critical point, the electrostatic force overcomes the surface tension of the solution and forms a jet. The electrically charged jet stretches and whips, transforming from a thin, long shape to hundreds of nanoscale fibers and rapidly evaporating. The dry fibers randomly accumulate on the surface of the metallic collector. The use of a rotating collector affords fibers with high mechanical strength. Similarly, the desired fiber properties can be obtained by aligning the fiber in the desired direction during the electrospinning process. In addition, through a continual electrospinning process (a polymer solution is continuously injected with an applied high voltage), the thickness of the fiber deposited on the collector surface can be adjusted. Hence, fibers with the desired diameter, structure, and morphology can be fabricated by adjusting various electrospinning parameters as shown in Figure 2 [11].

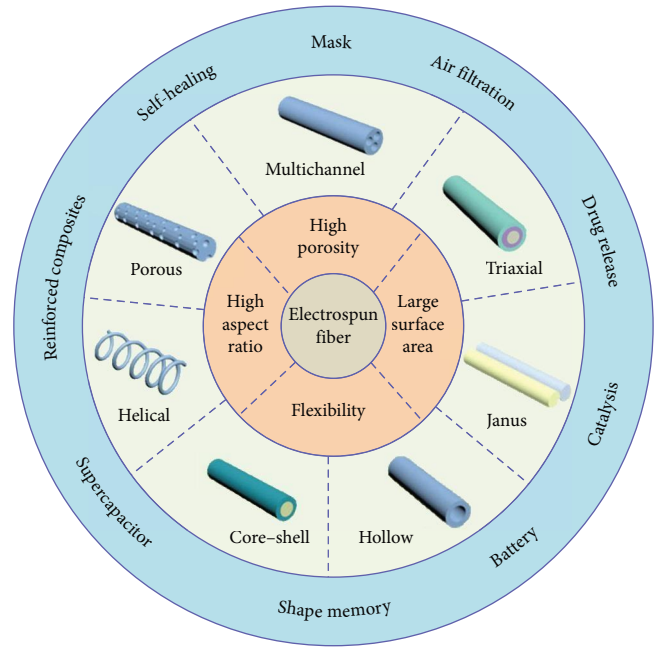

Figure 2: Characteristics and structures of electrospun fibers with different structural designs [10]. Copyright 2020 De Gruyter.

2.2. Different Electrospinning Parameters. To obtain the desired electrospun fibers, understanding the electrospinning parameters that affect the resultant material properties is essential. These parameters can be divided into three categories: solution parameters (solution concentration, viscosity, solvent, and solution conductivity); electrospinning parameters (the distance to the collector (DTC), voltage, flow rate, and needle diameter); and environmental conditions (relative humidity and temperature). Figure 3 shows a simple summary of the effects of parameters present in electrospinning and the variation of fiber diameter as a function of parameter. Changing these parameters can afford fine fibers, beaded fibers, or fibers with a rough surface. Moreover, a thin coating film can be obtained instead of a fiber. Therefore, in this section, we describe each electrospinning parameter to provide a better understanding of the electrospinning process.

2.2.1. Solution Parameter. The morphology of the nanofibers depends mainly on the initial polymer solution. Important factors such as polarity, viscosity, surface tension, and vapor pressure are affected by changes in the solution concentration, solvent, and molecular weight. Changes in these factors affect the nanofiber morphology and fiber diameter [12].

2.2.2. Solution Concentration. The viscosity depends on the concentration of the polymer solution. When the solution is lower than the optimal concentration, the polymer chains break owing to the applied surface tension and electric field. Therefore, an extremely low viscosity (low solution concentration) results in the formation of beads through an electrospray (Figure 4(a)) instead of an electrospun fiber. However, if a slightly higher concentration than the optimal concentration is used, the entanglement between the polymer chains increases, and these entangled chains overcome the surface

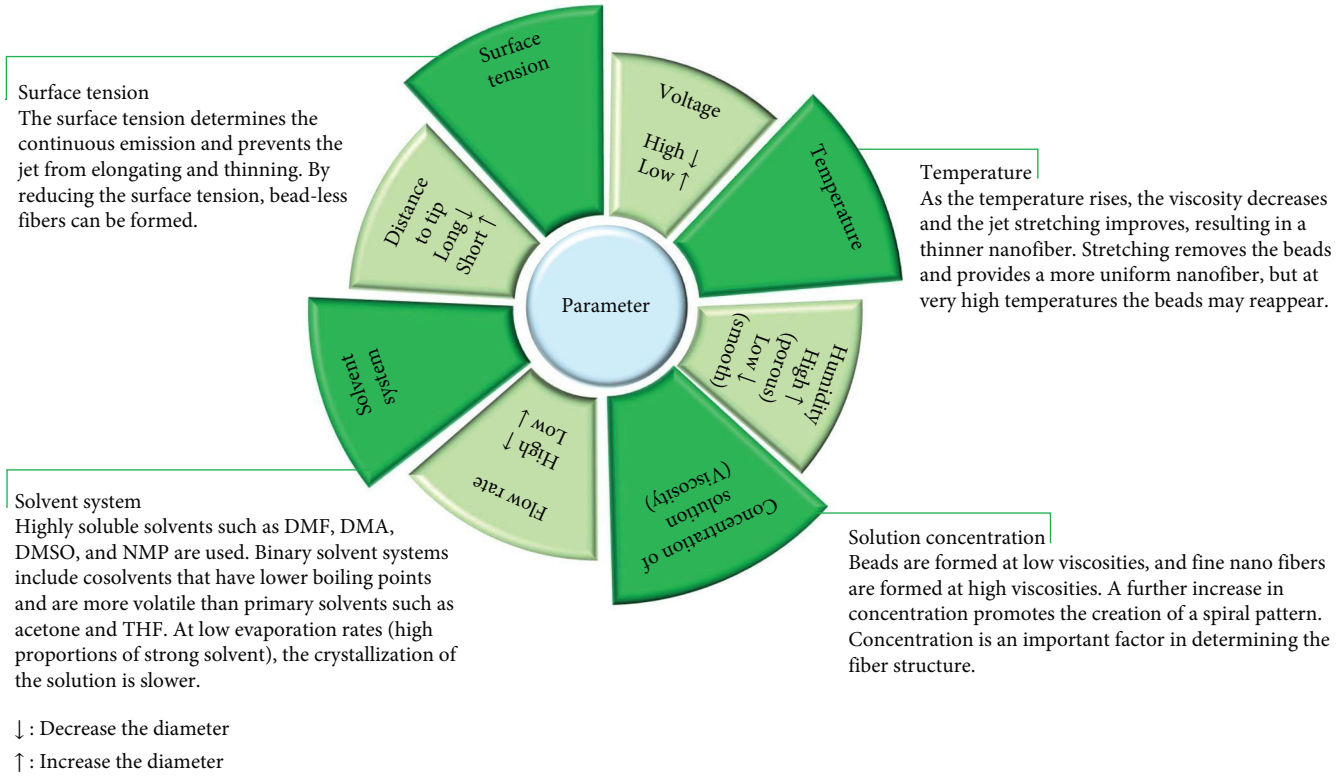

Figure 3: Parameters that affect fiber diameters during the electrospinning process.

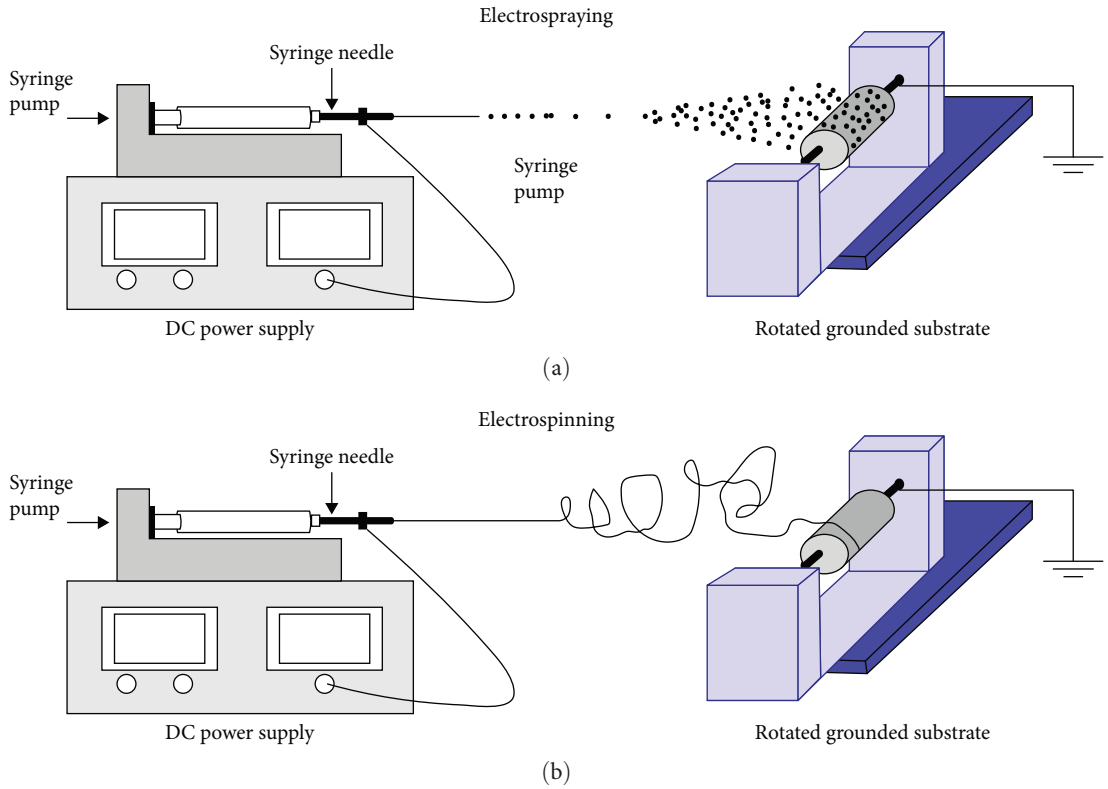

Figure 4: (a) Electrospraying and (b) electrospinning setup [13]. Copyright 2016 Taylor & Francis.

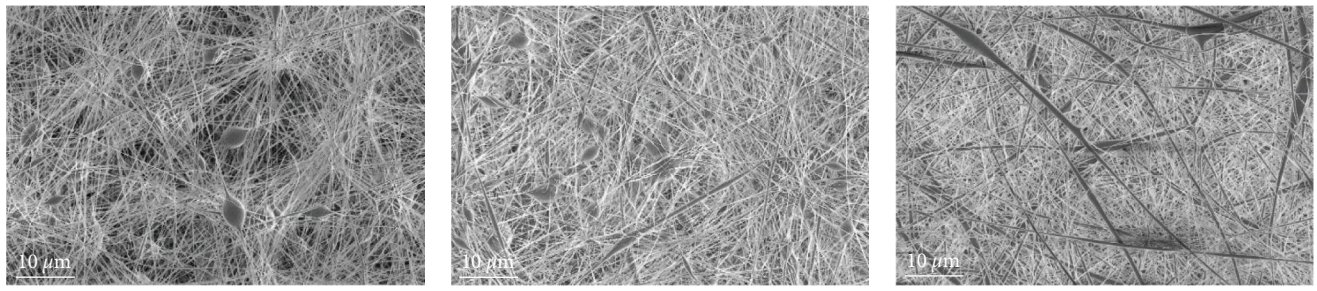

(a) (b) (c)

FIGURE 5: Scanning electron microscopy (SEM) images of polyvinylidene fluoride (PVDF) nanofibers prepared using (a) 12 wt%, (b) 15 wt%, and (c) 17 wt% PVDF solution.

tension, affording beads and fine nanofibers simultaneously. Only fine nanofibers are generated at the optimal concentration like Figure 4(b). However, helix-shaped microribbons appear at high solution concentrations (high viscosity). Therefore, determining the optimal solution concentration (viscosity) is essential in fabricating beadless fine nanofibers [13, 14, 15]. Figure 5 shows the experimental results of PVDF-based electrospinning as a function of solution concentration. At lower solution concentration, fibers with beads are formed, while at higher solution concentration, helix-shaped microribbons appear.

2.2.3. Solvent System. Solvents such as N,N-dimethylformamide (DMF), dimethylacetamide (DMA), dimethyl sulfoxide (DMSO), and N-methyl-2-pyrrolidone (NMP), in which polymers are highly soluble, are used in electrospinning. Acetone and tetrahydrofuran (THF) are used in binary solvent systems as cosolvents, which could help change the morphology and surface structure of the nanofibers. Acetone and THF are highly volatile cosolvents that serve to reduce the evaporation time of the solvent during spinning. Cosolvents can be used by itself, but because of low solubility, the solute does not dissolve well in the solvent, resulting in clogging of the syringe tip and inability to produce fine fibers. Therfore, because solvent systems determine the spinnability and the evaporation rate of the polymer solution, identifying a suitable volatile solvent for each solution is crucial. The solution crystallizes slowly at low evaporation rates (high solvent fraction). However, rapid crystallization results in insufficient time to form a stable phase. Therefore, a binary solvent system with an appropriate ratio of a main solvent with high solubility (DMF, NMP, DMSO, etc.) and a cosolvent with high volatility is required to produce fine fibers [16, 17].

2.2.4. Molecular Weight. The molecular weight of a polymer is also related to viscosity, which affects the morphology and diameter of the nanofibers. An optimal high-molecular-weight solution is used in electrospinning. Notably, the diameter of the fiber increases with increasing the molecular weight. A low-molecular-weight solution generates beaded fibers, whereas an extremely high-molecular-weight solution containing long polymer chains affords wrinkled fibers. Therefore, a polymer solution with the optimal molecular weight, which depends on the solute and solvent, is required to produce fine fibers [18].

2.2.5. Voltage. Voltage is a vital parameter for jet initiation and nanofiber formation in the electrospinning process. This is because the voltage directly affects the electric field intensity and the electric forces acting on the Taylor cone. Changes in the voltage affect the morphology, surface structure, diameter, and material properties of the fibers. A higher than optimal voltage affords thinner nanofibers owing to the stretching of the polymer solution, which correlates with charge repulsion within the polymer jet. Moreover, if a voltage higher than the critical voltage is applied, a Taylor cone is not fully formed, making it difficult to create a stable jet. This can result in beads or beaded fibers because most solvents do not evaporate completely in this case [19, 20, 21]. Figure 6 shows the experimental results of PVDF–HFP-based electrospinning as a function of voltage. It can be seen that as the voltage increases, the fiber diameter becomes smaller due to the stretching of the polymer solution.

2.2.6. DTC/Spinning Distance. The spinning distance is determined by the spinnability of the polymer solution and the evaporation rate of the solvent. In other words, DTC was adjusted according to the traveling time of the jet, fiber stretching, and the evaporation rate of the solvent. A control factor for the solvent evaporation ability is the use of a volatile solvent. Similarly, the evaporation time of the solvent can be controlled by the DTC. As the DTC increases, the distance for jet stretching increases and the time for the solvent to evaporate is increased from the fiber. However, as the DTC increases, the electric field decreases, so proper voltage control is required. Conversely, if the DTC is decreased, insufficient fiber stretching and solvent evaporation may occur, resulting in wet fiber formation or porous film. Changing the spinning distance does not typically play a significant role in nanofiber formation compared with other parameters. However, a proper DTC is required to produce fine fibers, and the voltage should be adjusted accordingly [22, 23].

2.2.7. Flow Rate (Feed Rate). Flow rate is one of the most critical parameters in the fabrication of nanofibers through electrospinning. This parameter affects the jet speed and rate at which the solution turns into a solid. When the flow rate fell below the critical point, no Taylor cones were formed. Conversely, unstable jets were formed if the flow rate was very high, which increased the droplets at the needle tip, affording fibers with low uniformity and decreasing the

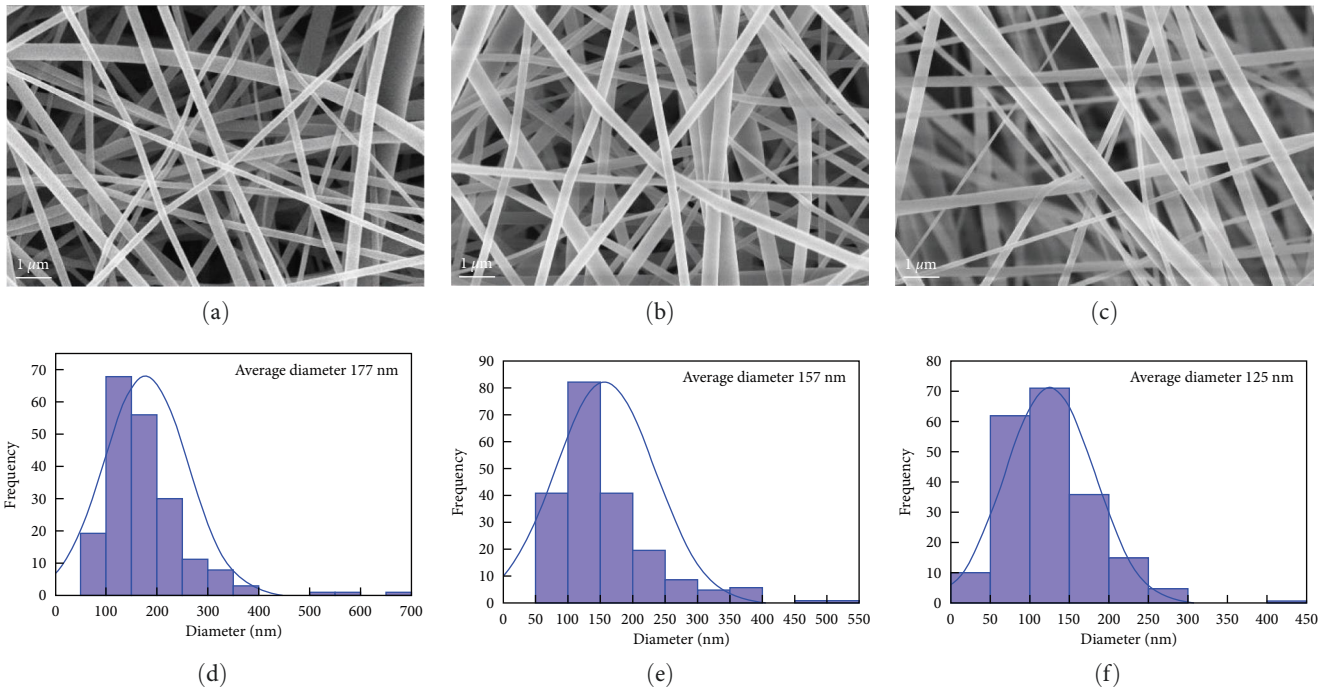

FIGURE 6: SEM image of poly(vinylidene fluoride-co-hexafluoropropylene) (PVDF-HFP) nanofiber fabricated using a voltage supply of (a) 10 kV, (b) 12 kV, and (c) 14 kV. The fiber diameter distribution of the PVDF-HFP nanofibers generated at (d) 10 kV, (e) 12 kV, and (f) 14 kV.

tensile strength of the polymer. In addition, a high flow rate resulted in an insufficient evaporation rate when the solution reached the collector, affording beaded fibers. Therefore, a slow flow rate is preferable to allow sufficient time for solvent drying and the polarization of the traveling jet [17, 24, 25].

2.2.8. Temperature. Electrospinning is typically conducted at room temperature. However, the ambient temperature varies depending on the season, which changes the viscosity, thereby affecting the electrospun fibers. As the ambient temperature increased, the viscosity decreased, leading to the formation of thinner nanofibers because of better jet-stretching. Although elongation removes beads and generates uniform fibers, the jet becomes unstable again at very high temperatures, leading to the formation of beads [26].

2.2.9. Relative Humidity. Humidity is a significant factor in determining the surface structure of the electrospun nanofibers. Smooth nanofibers were formed at average humidity, whereas porous nanofibers were generated at high relative humidity. In addition, at high relative humidity, the condensed water on the fiber surface dried slowly and the number of merged droplets increased, resulting in a macroporous structure. Solvent evaporation, which affects the spinnability of polymer solutions, is also related to humidity. For example, the solvent evaporates rapidly in a dry environment, hindering the jet path [27, 28, 29]. Based on the above principle, the results of the effect of humidity on PVDF-based electrospinning in Figure 7 show that as the humidity increases, the macroporous structure of the fibers appears.

Except for the above parameters, there are various parameters such as syringe and nozzle type, syringe nozzle diameter, additive, dielectric constant, etc. Therefore, the advantage of electrospinning is that you can create the desired fiber morphology, structure, and diameter by controlling these parameters.

2.2.10. Advantages of Using Electrospun Nanofibers in LIBs. LIBs are rechargeable lightweight batteries, usually operated at 4 V, and have an energy density of 120–200 $W{\cdot}hr{\cdot}kg^{-1}$ and a power density of 250–1,000 $W{\cdot}kg^{-1}$ [30]. Even though LIBs are a promising solution for overcoming the global energy problem, many practical challenges must be overcome in devices such as EVs and HEVs that require large-capacity ESS. Improving the electrochemical performance and stability of LIBs is one such issue. Various methods such as solid-state reactions, coprecipitation, molten salt synthesis, pulsed laser deposition, and electrospinning have been used to improve the performance of LIBs. The incorporation of a 1-D structure synthesized via electrospinning in LIBs is a simple and inexpensive method. The continuous fibrous morphology of an electrospun nanostructure would shorten the diffusion pathway of Li ions, achieving rapid Li-ion intercalation/deintercalation. Moreover, the highly porous nanostructure provides a high surface area. These characteristics improve the stability and electrochemical performance of the LIBs. In addition, increasing the mechanical strength of the electrospun nanofibers could improve battery safety.

3. Electrospun Nanofibers as Cathode Materials

The cathode (positive electrode) plays an important role in maintaining the specific capacity of a battery. LIB cathodes should preferably exhibit high energy density and stability and be inexpensive. However, Li, which is a common LIB cathode material, is unstable and expensive; therefore, Li

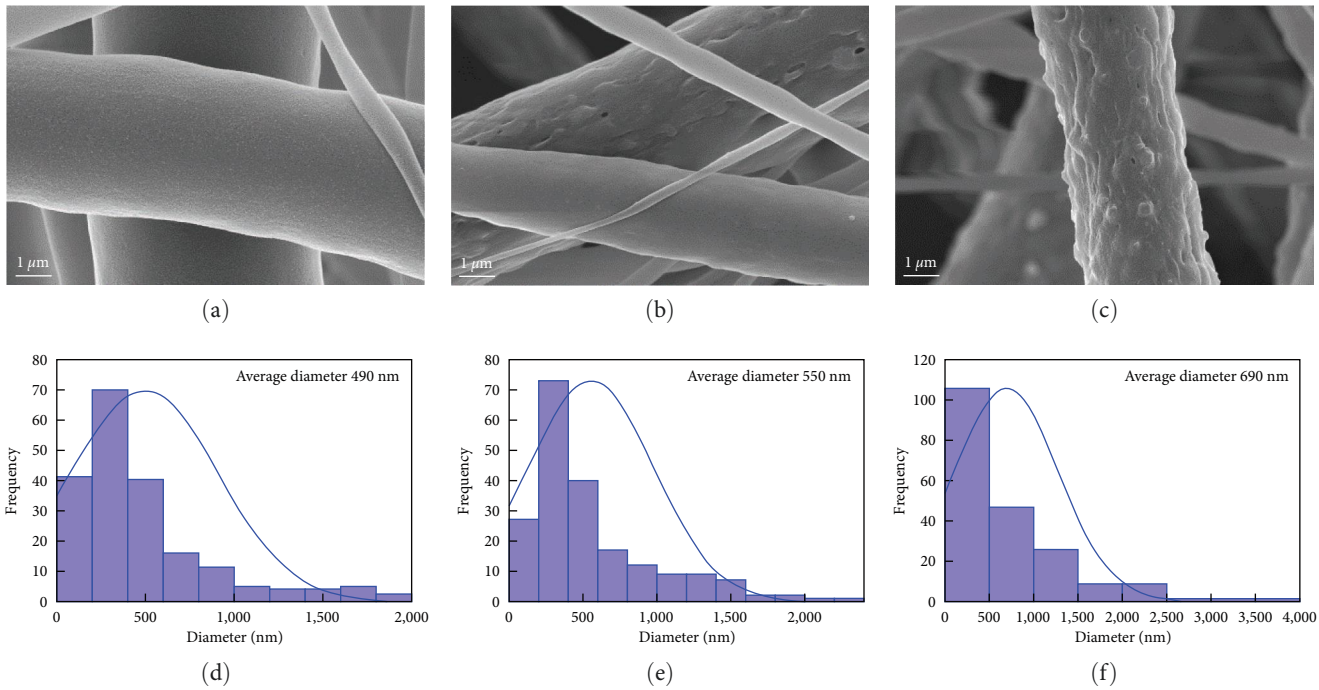

FIGURE 7: SEM image of PVDF nanofibers fabricated at (a) 35% relative humidity (RH) at an average diameter of 490 nm, (b) 55% RH at an average diameter of 550 nm, and (c) 75% RH at an average diameter of 690 nm; fiber diameter distribution of PVDF nanofibers fabricated at (d) 35% RH, (e) 55% RH, and (f) 75% RH.

complexes with other metal oxides (V, Fe, Co, Ni, phosphates, and transition metals such as Mn) have been used in LIBs to increase their stability [31]. In conventional LIBs, Li metal oxide powder has a long diffusion path for Li-ion intercalation/deintercalation cycles, which reduces the reaction rate of the Li ions. This contributes to the deterioration of the electrochemical performance of LIBs. One solution to these problems is to use 1-D electrospun nanofibrous structures.

Currently, $LiCoO_2$ is the most widely used cathode material for LIB because of its facile preparation, stable electrochemical cycling, high theoretical specific capacity (274 $mA{\cdot}hr{\cdot}g^{-1}$), and high theoretical energy density (140 $mA{\cdot}hr{\cdot}g^{-1}$). However, only ~50% of the Li ions in $LiCoO_2$ cathodes participate in the reaction, resulting in performance degradation, high costs, low structural and thermal stability, and toxicity [32, 33]. $LiMn_2O_4$ is an environment friendly cathode material with high cycle performance at room temperature and excellent rate performance due to 3D Li^+ diffusion channel. And its theoretical capacity is 148 $mA{\cdot}hr{\cdot}g^{-1}$, and a practical capacity of 110–120 $mA{\cdot}hr{\cdot}g^{-1}$ at 3.0–4.2 V range; moreover, it is inexpensive and has abundant resources [34, 35]. However, owing to the Jahn–Teller effect, $LiMn_2O_4$ undergoes a tetragonal lattice change in the cubic phase during high rate discharge, which destroys its structural integrity. This problem increases with increasing temperature [36]. To solve this problem, $LiMn_2O_4$ porous nanofibers were synthesized via electrospinning. Compared to $LiMn_2O_4$ nanoparticles, $LiMn_2O_4$ nanofibers demonstrated improved stability and rate performance as a cathode material. Furthermore, the $LiMn_2O_4$ nanofiber cathode provides a larger surface area and a shorter diffusion path to Li ions and has a "network-like" structure, thus enhancing the electrochemical performance and cycle stability of the LIBs [37].

However, Mn causes the Jahn–Teller effect and dissolves in the electrolyte, leading to the structural deterioration of the cathode. To overcome this issue, Ni-doped $LiMn_2O_4$ ($LiNi_{0.5}Mn_{1.5}O_4$), which exhibits a very high working voltage and structural stability, was developed. Spinel $LiNi_{0.5}Mn_{1.5}O_4$ can reach a high energy density of 658 $W{\cdot}hr{\cdot}kg^{-1}$ owing to the redox transformation of Ni^{4+} to Ni^{2+} at 4.7 V; the energy density of pristine $LiMn_2O_4$ is 440 $W{\cdot}hr{\cdot}kg^{-1}$. $LiNi_{0.5}Mn_{1.5}O_4$ also exhibited a discharge capacity of 133 $mA{\cdot}hr{\cdot}g^{-1}$ and a coulombic efficiency of 93% at 0.5 C. At a rate of 0.5 C, the stable discharge capacity was 130 $mA{\cdot}hr{\cdot}g^{-1}$, which slightly decreased to 124 $mA{\cdot}hr{\cdot}g^{-1}$ after 30 cycles as shown in Figure 8; the coulombic efficiency was maintained at over 90% during charge–discharge cycles [38].

In addition, attempts to replace $LiCoO_2$ are currently underway. The development of NCM (Ni + Co + Mn) cathode materials is a hot research topic in this area, as they contain fewer amounts of the relatively expensive Co and exhibit higher thermal stability. In addition, these mixed materials can demonstrate better cathode performance than single-component cathodes owing to the synergistic effect of Ni, Co, and Mn. $Li(Ni_xCo_yMn_{1-x-y})O_2$ shows high specific capacity, conductivity, and safety. However, NCMs have certain disadvantages. Because of their complex structures, serious cation disorders occur, leading to large capacity degradation and stability problems [39]. To solve this issue, Zhou et al. [40] synthesized a core–shell Li (NCM) oxide metal cathode (Figure 9(a)) through electrospinning using lithium, cobalt,

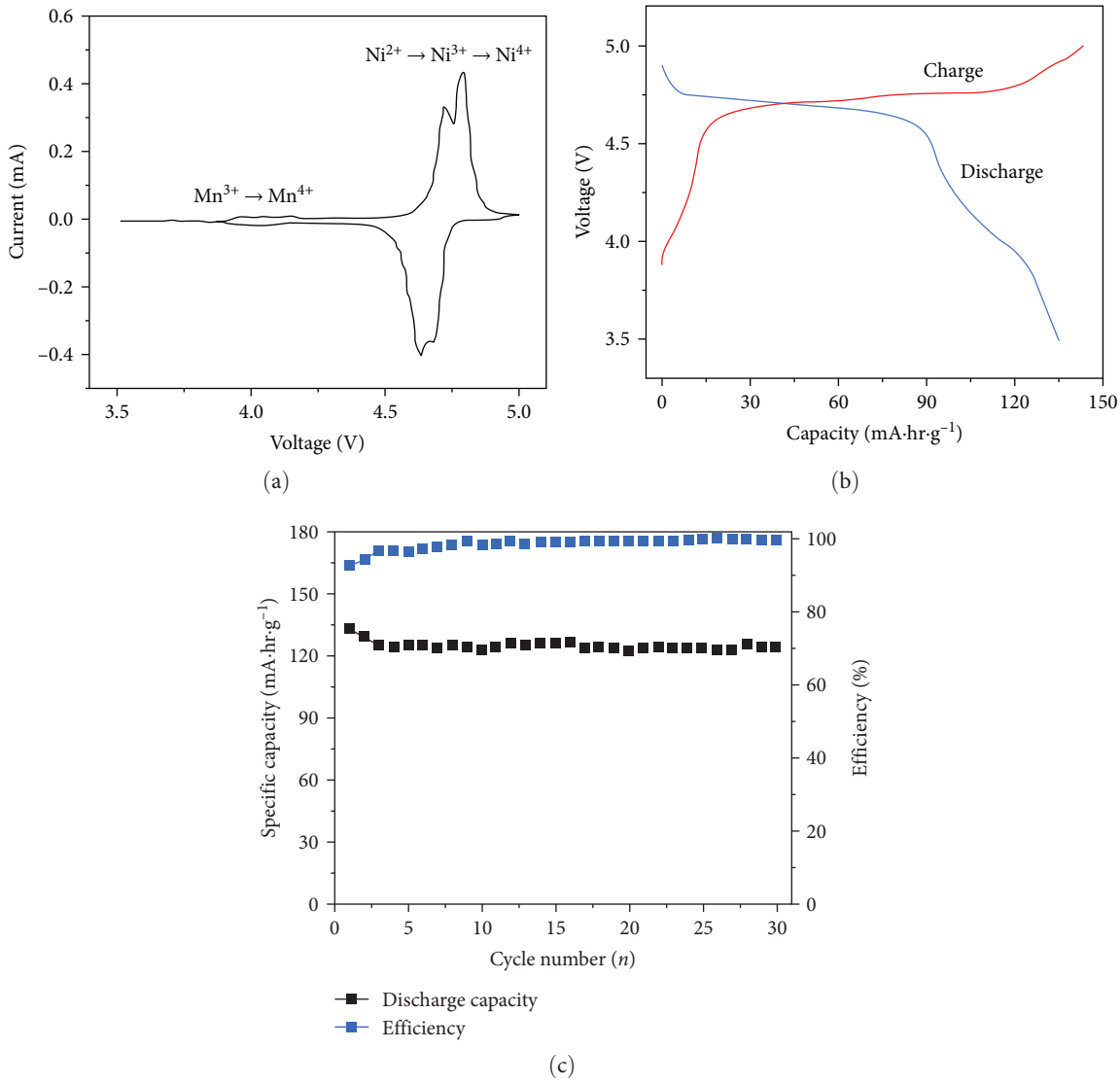

FIGURE 8: (a) Cyclic voltammograms at a scanning rate of 0.18 mV·s^{-1}, (b) galvanostatic discharge/charge profiles at 0.5 C, and (c) cycling performance at a 0.5 C of the hierarchical nanofibers of $LiNi_{0.5}Mn_{1.5}O_4$ [38]. Copyright 2013 Wiley Online Library.

nickel, and manganese acetate for starting materials to provide metal cations and environment-friendly citric acid with high decomposition temperature as a chelating agent. The high initial charge and discharge capacities of this fiber were 211.2 and 195.7 mA·hr·g^{-1} (Figure 9(b)), respectively. Moreover, these ternary cathodes exhibited enhanced structural and electrochemical stability (Figure 9(c)) [40].

Lv et al. [41] reported enhanced LIB performance with Nb-doped NCM nanofiber cathode prepared via electrospinning. Electrochemical polarization was alleviated by Nb doping, and the diffusion coefficient of the Li ions increased. This LIB also showed high reversible capacity and high discharge capacity at even high current rate as shown in Figure 10 [41].

Ding et al. [42] developed Al-doped Li (NCM) oxide nanofibers using a sol–gel electrospinning process. Al improved the reversible capacity and cycling performance of $Li(NCM)O_2$. In detail, the substitution of Mn^{4+} ions by Al^{3+} ions increases the content of low valence transition metal ions, which improves the structural stability. Al-doping reduced the amount of Mn, and the highest initial discharge capacity of the corresponding LIB was 186.59 mA·hr·g^{-1} at 0.1 C when the Ni : Co : Mn : Al ratio was 1 : 1 : 0.82 : 0.18. A capacity retention of 96.1% was observed after 30 cycles [42].

An NCA (Ni + Co + Al) nanofiber cathode was introduced to reduce the cost while increasing the electrochemical and safety performance of $Li(NCM)O_2$. The Al content was very low in this ternary system [43], and unlike Mn^{4+}, Al^{3+} does not change its valence state during electrochemical cycling, which reduces the cost of the cathode and improves the structural stability of the material. The NCA nanofibers (Figures 11(a) and 11(b)) exhibited a high discharge capacity of 206.4 mA·hr·g^{-1} at 0.1 C and a capacity retention of 81.5% after 100 cycles at

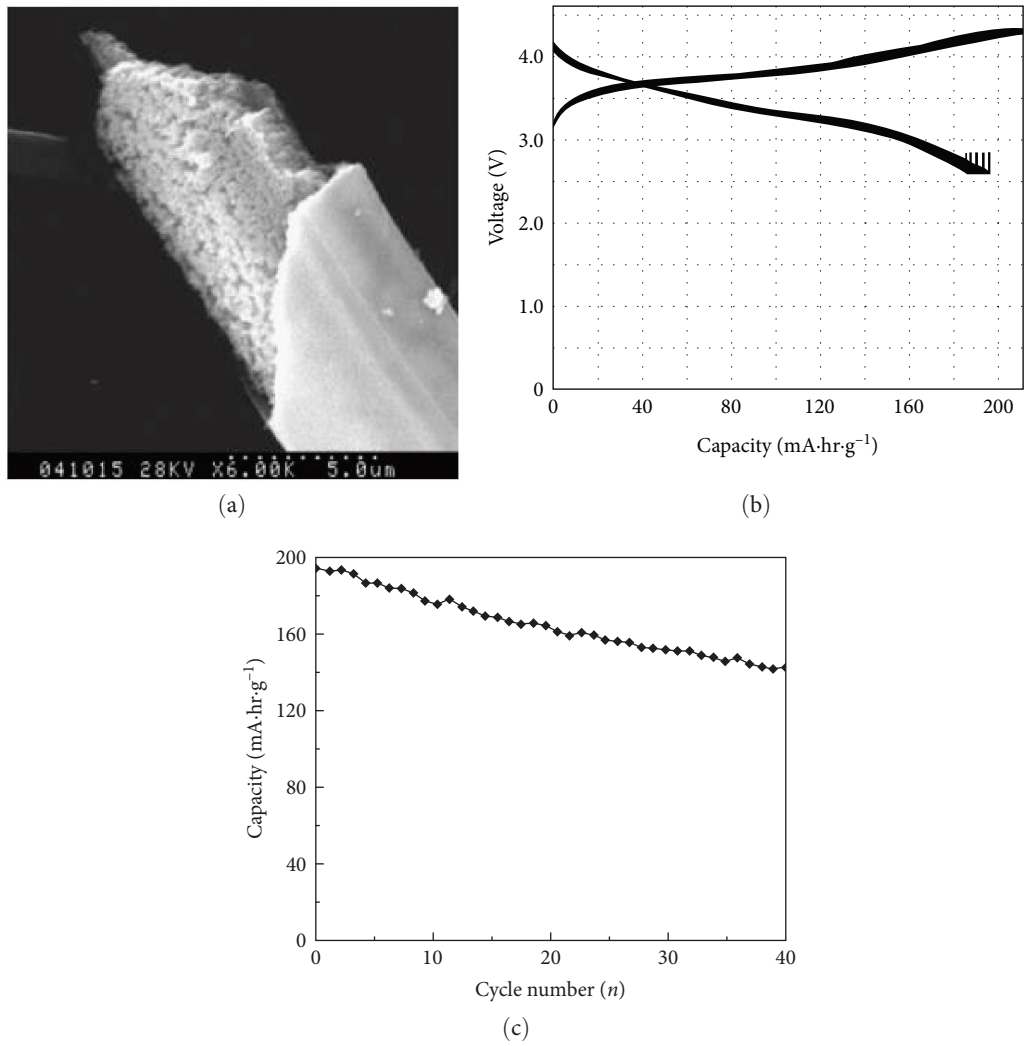

FIGURE 9: (a) SEM images of the calcined fibers, (b) charge/discharge curves, and (c) cycle performance of $Li(Ni_{1/3}Co_{1/3}Mn_{1/3})O_2/Li(Ni_{1/2}Mn_{1/2})O_2$ fibers [40]. Copyright 2010 Elsevier.

0.5 C as shown in Figures 11(c) and 11(d). In addition, it exhibited stability while maintaining good fiber structure even during cycling [44].

Thus, using a fibrous-structure cathode prepared through electrospinning can reduce the diffusion path of Li ions and improve their diffusion coefficient. In addition, the fibrous structure increases the contact area between the electrolyte and active particles and reduces the aggregation of active particles; therefore, it significantly improves the structural and electrochemical performance of the corresponding LIBs.

4. Electrospun Nanofibers as Anode Materials

The anode (negative electrode) also affects the energy density, stability, and rate performance of an LIB; moreover, it also affects Li consumption, causes irreversible electrolyte reactions, slows lithium intercalation, and causes dendrite formation owing to the formation of a solid electrolyte interphase (SEI) [45, 46]. The anode materials used in commercial LIBs should be inexpensive, have good specifications, and be available in large amounts. Graphite is the most common anode material for LIBs. However, graphite exhibits a low theoretical capacity (372 mA·hr·g^{-1}), cycle instability, low rate capability, and Li dendrite formation by intercalation and deintercalation through the internal basal plane of the anisotropic graphite microstructure [47]. This problem can be solved by increasing the theoretical capacity by creating additional space for Li ions or increasing the surface-to-volume ratio of the material to improve the rate capability and safety [48]. LIBs with high energy density, high safety, and fast charging can be achieved by making structural changes to the existing materials.

The lithium-storage mechanism in the anodes of rechargeable LIBs can be divided into three types: insertion or intercalation, conversion, and alloying. Figure 12 simply represents the lithium storage mechanism for the three anode types. Insertion involves inserting and extracting Li ions without structural changes in the microstructure. Graphite (theoretical capacity = 372 mA·hr·g^{-1}) and $Li_4Ti_5O_{12}$ (theoretical capacity = 175 mA·hr·g^{-1}), which are structurally very small and safe,

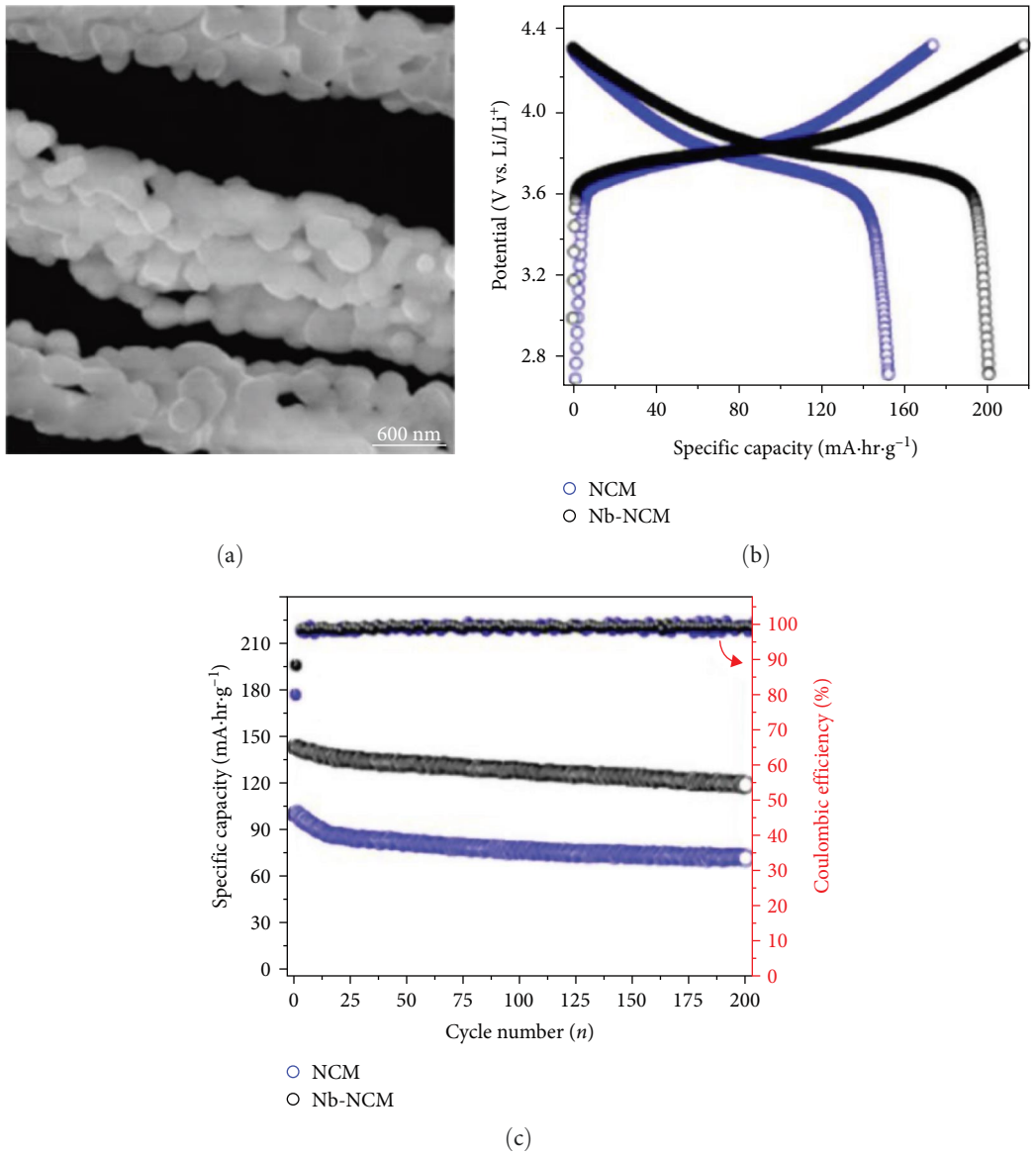

FIGURE 10: (a) SEM image of electrospun Nb-NCM nanofibers, (b) initial charge and discharge curves at 1 C, and (c) cycling performance of Nb-NCM and NCM electrodes at 5 C [41]. Copyright 2019 Elsevier.

are commonly used for insertion type. However, this method results in a theoretically low capacity. Conversion is a method of storing Li ions while changing the ionic bonding between Li ions and other metallic cations and anions, such as metal oxides, metal sulfides, and metal selenides. Fe_2O_3 and NCM are common materials used for conversion. They have the advantage of a higher theoretical capacity than that obtained from insertion, but have the disadvantages of poor kinetics and large volume changes. Finally, alloying is a method in which Li ions are alloyed with a host metallic phase while breaking the internal atomic bonds of the host material. Si and Ge are common materials used for alloying and lead to a high specific capacity and low working potential; however, these alloys have the disadvantages of very large volume changes, pulverization, SEI growth, and electrical contact loss [49, 50, 51, 52].

4.1. Insertion. Graphite, amorphous carbon materials, and Ti-based materials are usually used as anodes and have a layered or 3-D network structure. The insertion-type mechanism has the advantages of a very small volume change, good structural stability, and a long cycle life during electrochemical reactions.

Graphite is the most common anode material because of its low price, abundance, relatively high gravimetric capacity ($372\ mA{\cdot}hr{\cdot}g^{-1}$) and low working potential (0.2 V) [53]. However, owing to their low working potential, Li dendrites can easily form on graphite surfaces. It also has the disadvantage of having a lower theoretical capacity than Si-based materials and Li–metal anodes [54, 55]. One way to overcome this problem is to use 1-D structures such as carbon nanofibers (CNFs) or carbon nanotubes (CNTs), which increase the

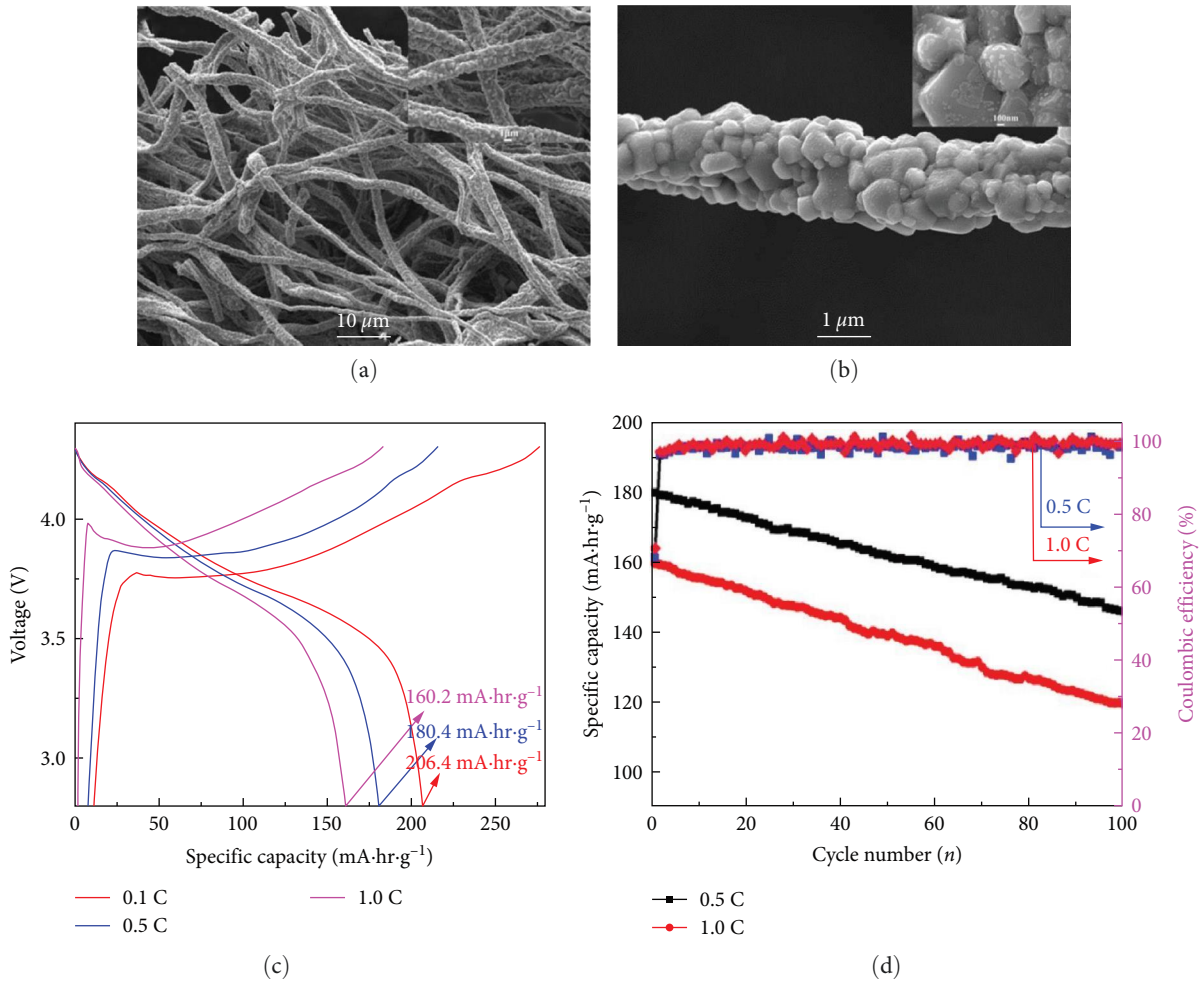

Figure 11: (a, b) SEM images of NCA fibers; (c) initial charge/discharge profiles of the NCA fibers at 0.1C; and (d) cycling performance of the NCA fibers at 0.5 C and 1 C [44]. Copyright 2020 iopscience.

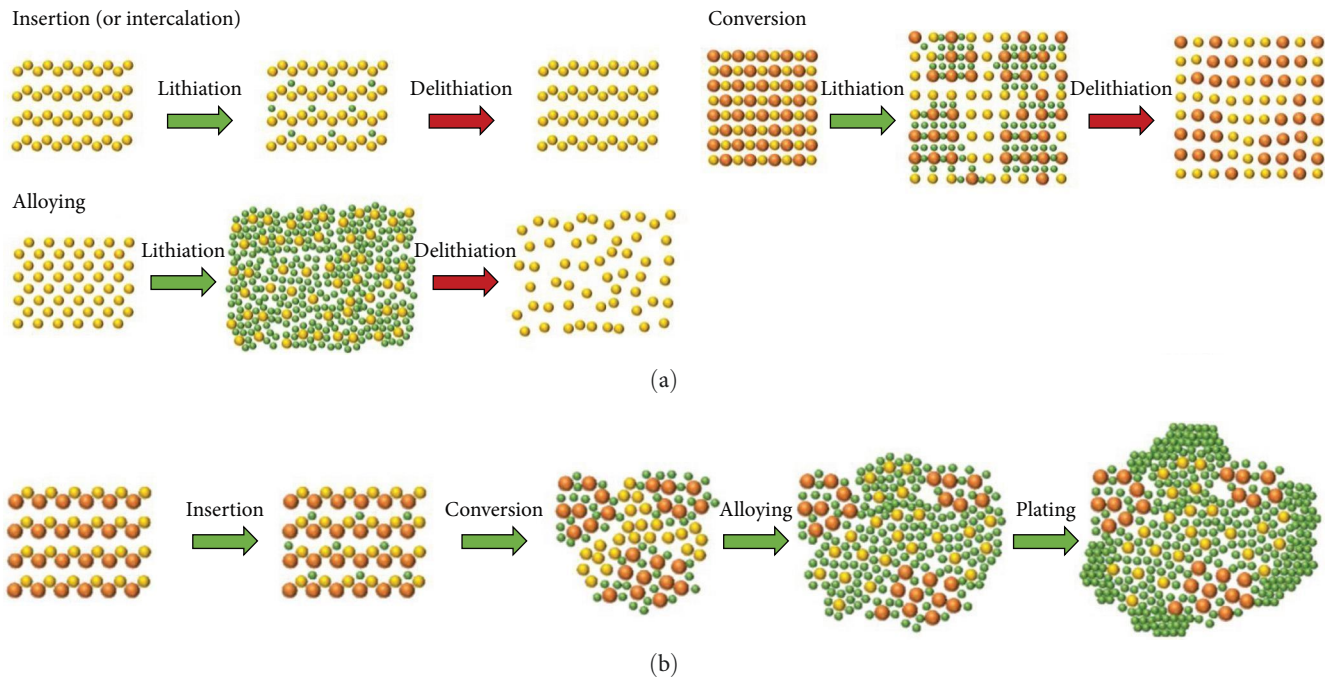

Figure 12: Schematic diagram of (a) basic Li-storage principles of the anode materials and (b) microstructural change of ceramic materials during the stepwise lithiation processes [49]. Copyright 2020 mdpi.

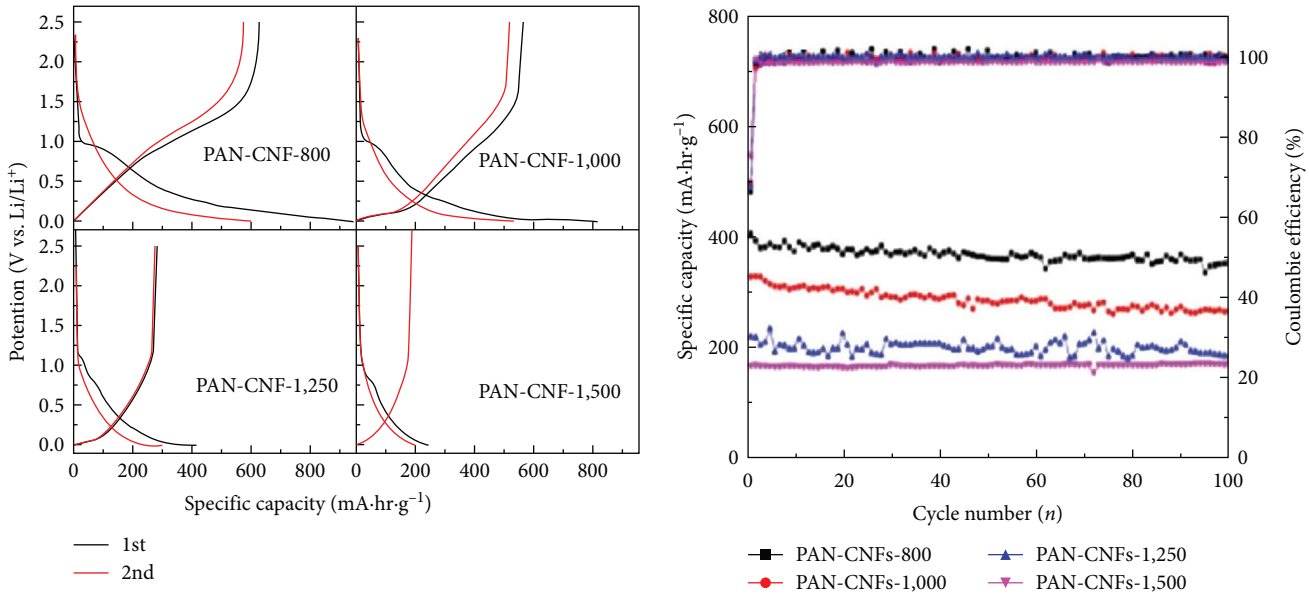

FIGURE 13: (a) Galvanostatic charge/discharge profiles of PAN-CNFs-800, PAN-CNFs-1,000, PAN-CNFs-1,250, and PAN-CNFs-1,500 in LIBs during the initial two cycles between 0 and 2.5 V at a current density of 0.02 $A \cdot g^{-1}$ and (b) cycle performances and Coulombic efficiencies of the PAN-CNFs anodes at a current of 0.1 $A \cdot g^{-1}$ in LIBs [57]. Copyright 2014 Elsevier.

surface-to-volume ratio. An easy and inexpensive way to make such a 1-D structure is electrospinning. The CNF mesh obtained through electrospinning is very flexible and exhibits improved electron transfer [56].

Jin et al. [57] prepared electrospun CNTs using a PAN solution via carbonization at different temperatures between 800 and 1,500°C. Owing to the high N content of PAN, N was doped *in situ* into CNF, which helped to improve the conductivity and provide additional Li-ion storage space. As shown in Figure 13, the reversible capacity of CNF that was carbonized at 1,250°C was 271 $mA \cdot hr \cdot g^{-1}$, and the initial coulombic efficiency was 72%; a 99% capacity retention was observed even after 100 cycles at 100 $mA \cdot hr \cdot g^{-1}$ [57].

CNTs with a porous structure provide not only a reservoir for Li-ion adsorption but also an effective diffusion method while increasing the distribution and number of active sites. Zhu et al. [58] fabricated graphitized porous CNFs (GPCNTs) using three heat treatments and demonstrated differences in the electrochemical performances of the GPCNTs calcined for different times between 3 and 18 hr. The GPCNTs achieved a capacity of 473.5 $mA \cdot hr \cdot g^{-1}$ after 100 cycles at 0.5 $A \cdot g^{-1}$ [58].

Furthermore, doping the porous carbon matrix with other materials such as B, N, and P improves the Li-storage capacity of carbon-based anodes [59]. Tong et al. [60] fabricated porous nanofibers with a very large surface area that enables an optimal electrode/electrolyte interface for Li adsorption. The micro–mesopores transport ions rapidly and serve as a reservoir for Li-ion storage. In addition, high heteroatom doping improves the electrochemical reactivity, electron conductivity, and Li-storage capacity of the carbon-matrix anode. CNFs with PE oxide@PAN and PVP core–shell structures were fabricated, and their LIB performance was improved by 10.2% N-doping. As shown in Figure 14, at 0.2 $A \cdot g^{-1}$, the very high initial capacitance (965.3 $mA \cdot hr \cdot g^{-1}$) decreased to 650.9 $mA \cdot hr \cdot g^{-1}$ at the 5th cycle and then increased to 820.3 $mA \cdot hr \cdot g^{-1}$ at the 220th cycle. After that, it showed excellent cycle performance, remaining at 820.3 $mA \cdot hr \cdot g^{-1}$ until 500 cycles. While the conventional carbon fiber showed an efficiency of 92.7% of the initial capacitance after 30 cycles, the carbon fiber with N-doped core–shell structure showed an excellent coulombic efficiency of 99% after 30 cycles and beyond [60].

4.2. Conversion. High-specific-capacity, low-cost, and nontoxic transition metal oxides have been used as anode materials for conversion. Representative materials such as Fe_2O_3, Fe_3O_4, NiO, and MnO have been used in many studies to increase the anode capacity. The conversion-type anode undergoes a reversible redox reaction with Li ions to generate nanoscale metal elements and Li compounds for the storage and release of Li ions. Conversion-type anodes have higher theoretical capacities than insertion-type anodes because they enable high electron transfer. However, despite their high specific capacities, transition metal oxide anode materials suffer from pulverization, electrical contact loss, and fewer Li ion diffusion pathways owing to microstructural rearrangements and large volume changes. However, the 1-D structure derived from electrospinning provides short diffusion paths and axially connected electronic pathways, similar to those observed for insertion-type anodes, thus accelerating the movement of Li ions and electrons [61, 62, 63].

Qin et al. [64] fabricated porous carbon nanofibers (PCNFs) via Fe_3O_4 encapsulation (Figure 15(a)). At 0.2 $A \cdot g^{-1}$, the initial reversible capacity was 1,015 $mA \cdot hr \cdot g^{-1}$, and the capacity

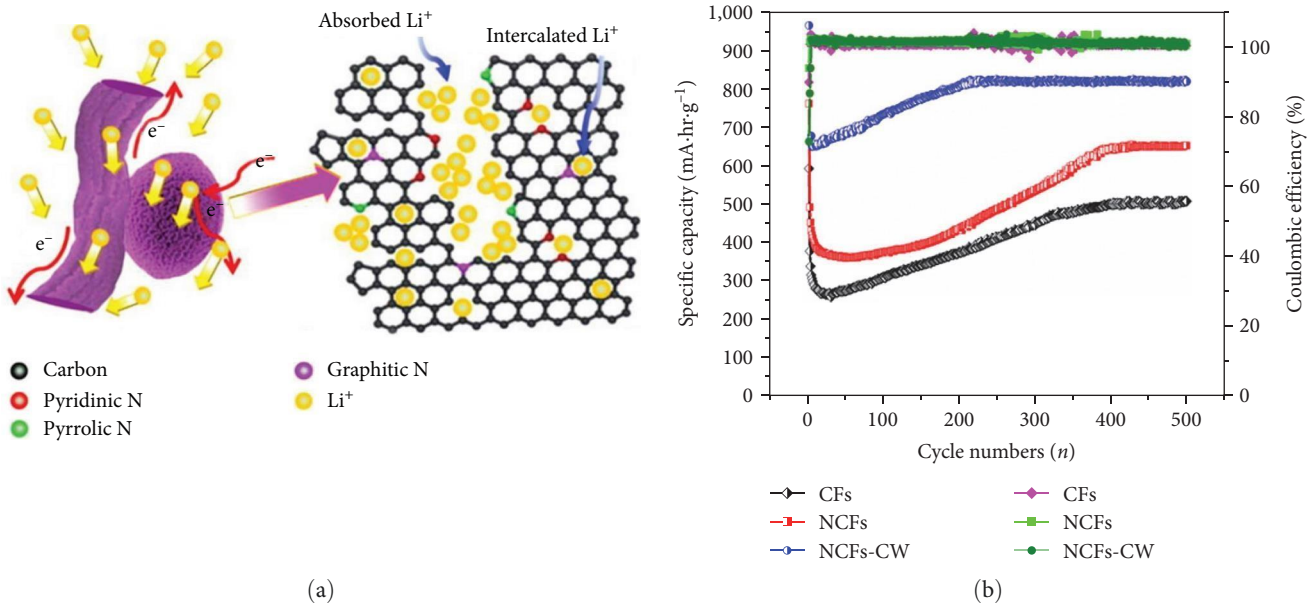

FIGURE 14: (a) Schematic diagram of the core–shell structure of GPCNTs and (b) cycling stability of the samples over 0.01–3.0 V (vs. Li+/Li) at 0.2 $A \cdot g^{-1}$ [60]. Copyright 2021 Elsevier.

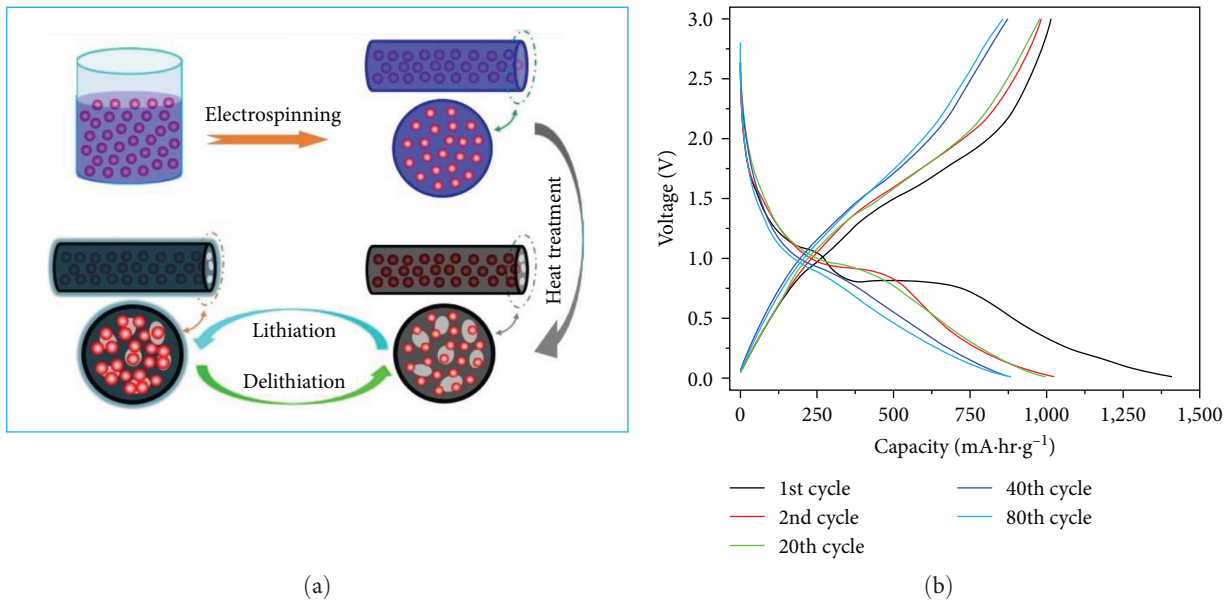

FIGURE 15: (a) Schematic diagram of the preparation process and structure of Fe_3O_4@PCF; (b) charge/discharge profiles of Fe_3O_4@PCF anodes at a current density of 0.2 $A \cdot g^{-1}$ for the 1st, 2nd, 20th, 40th, and 80th cycles [64]. Copyright 2015 Elsevier.

retention was 84.4% after 80 cycles and 91% after 200 cycles (Figure 15(b)) [64].

Zhu et al. [65] synthesized 1-D $MnCo_2O_4$ hollow-structure nanotubes with the spinel phase of AB_2O_4. These nanotubes exhibited a high rate performance of 400.4 $mA \cdot hr \cdot g^{-1}$ at 1 $A \cdot g^{-1}$ with a very high specific capacity of 701.4 $mA \cdot hr \cdot g^{-1}$ even after 300 cycles at 500 $mA \cdot g^{-1}$. The 1-D hollow nanotube structure connected to these $MnCo_2O_4$ particles significantly increased the number of active sites, reduced the Li diffusion length, and alleviated the pulverization problem caused by volume change [65].

Wang et al. [66] synthesized ternary/mixed $NiCoO_2$ nanofibers via electrospinning and annealing of the nanostructures and achieved high specific capacity and high rate capability. This hierarchical nanoparticle–nanofiber structure (Figure 16(a)) provided an expanded active surface area for buffering the volume change and Li storage during the lithiation/delithiation process and facilitated charge/electrolyte

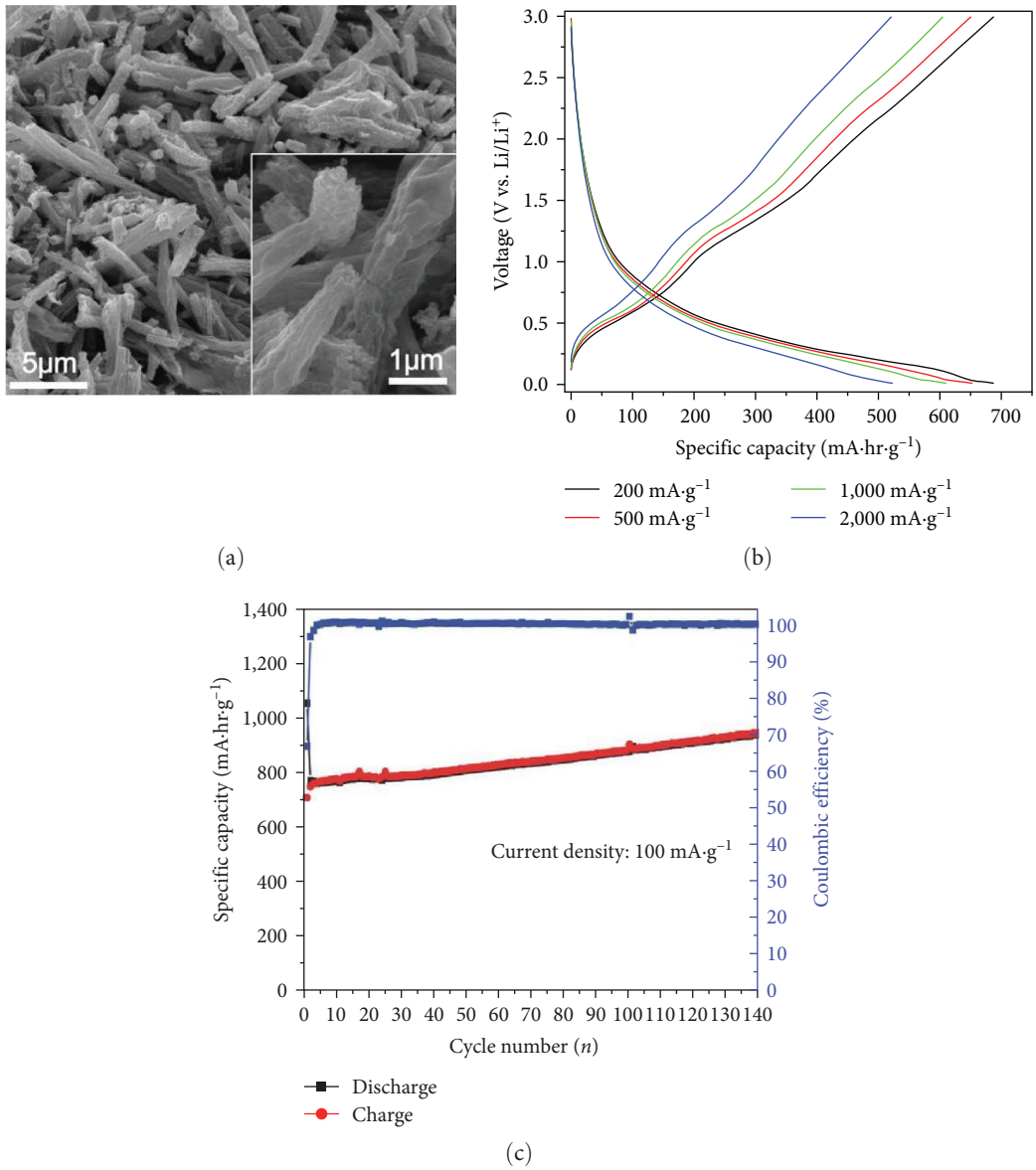

FIGURE 16: (a) SEM images of the $NiCoO_2$ nanofibers; (b) galvanostatic discharge/charge profiles at different rates ranging from 200 to 2,000 $mA{\cdot}hr{\cdot}g^{-1}$; and (c) cycling performance along with corresponding Coulombic efficiency at 100 $mA{\cdot}g^{-1}$ [66]. Copyright 2019 Wiley.

diffusion. It showed a very high discharge capacity of 945 $mA{\cdot}hr{\cdot}g^{-1}$ after 140 cycles at 100 $mA{\cdot}g^{-1}$ (Figure 16(c)) and a high rate capacity of 523 $mA{\cdot}hr{\cdot}g^{-1}$ at 2,000 $mA{\cdot}g^{-1}$ (Figure 16(b)) [66].

4.3. Alloying. The alloying-type anodes can lead to very-high-energy-density batteries owing to the very high theoretical capacity and relatively low working potentials of the materials used. The anode materials used for alloying are Si (4,212 $mA{\cdot}hr{\cdot}g^{-1}$ and <0.5 V), Sn (992 $mA{\cdot}hr{\cdot}g^{-1}$ and ≤0.8 V), Ge (1,626 mAh g^{-1} and <0.5 V), and Sb (660 mAh g^{-1} and <1.0 V) [67, 68, 69, 70, 71, 72, 73, 74]. Alloying-type anodes exhibit reversible lithiation/delithiation through Li alloying/dealloying reactions when Li is stored. The equation for this reaction is: $M + xLi^+ + xe^- \leftrightarrow Li_xM (0 \le x \le 4.4, M = Si, Ge, etc.)$ [75]. Similar to conversion-type anodes, alloying-type anodes suffer from issues such as structural degradation, SEI formation, electrical contact loss, and rapid specific capacity decay owing to large volume changes during the Li insertion/extraction process.

The most commonly used material in alloying-type anodes is Si, which has a very good specific capacity (4,212 $mA{\cdot}g^{-1}$) and a relatively low lithiation potential (0.4 V vs. Li/Li^+); moreover, it is an economic material owing to its abundance on earth [76]. However, Si continues to expand in volume during the lithiation process, generating cracks in the formed SEI and leading to pulverization. However, the exposure of the electrode surface to the electrolyte regenerated the SEI. This not only consumes a very large amount of electrolyte but also increases the diffusion distance of Li ions, reducing the coulombic efficiency and causing electrode deterioration [77]. Nevertheless, nanoscale structural changes in the Si

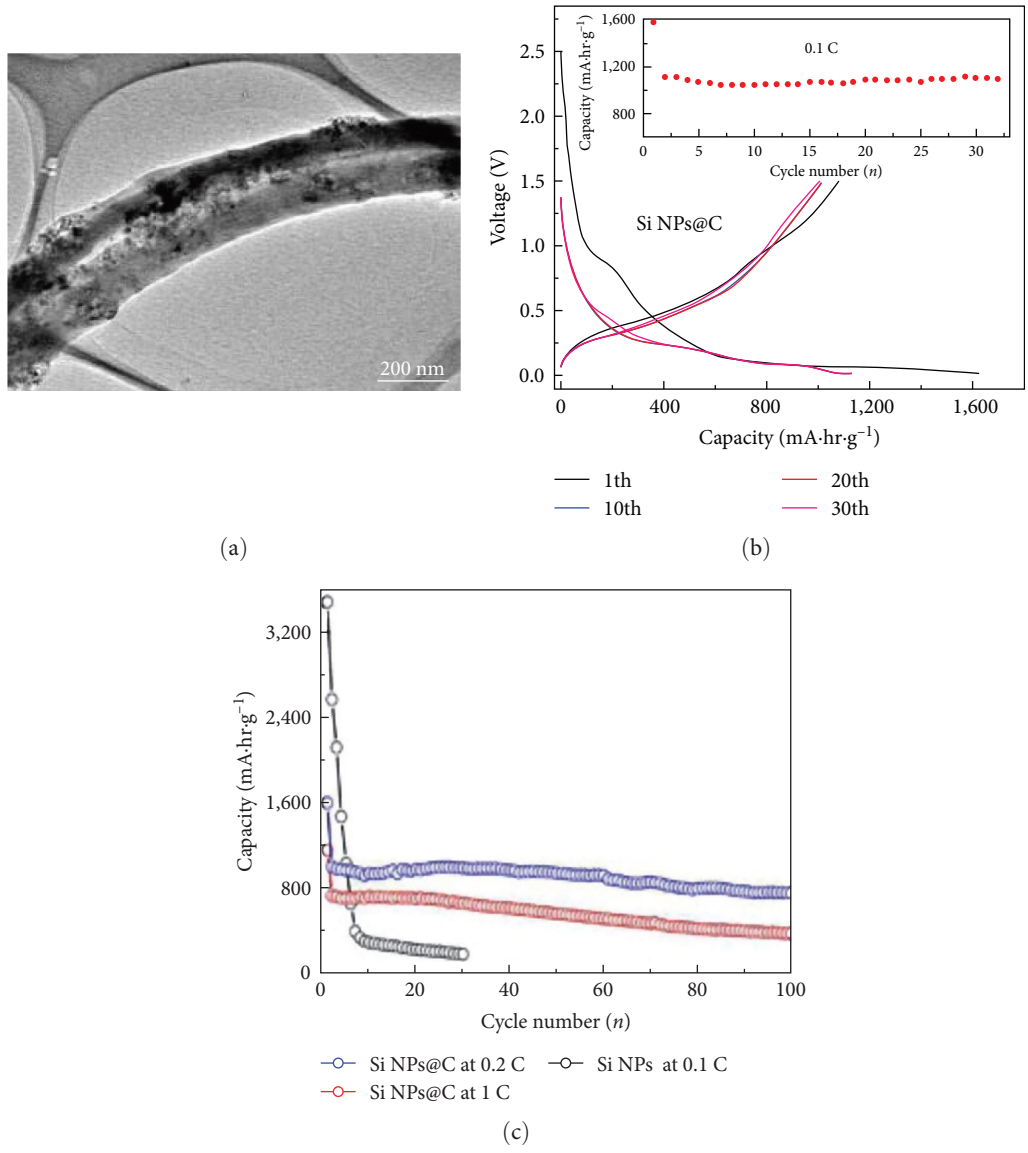

FIGURE 17: (a) TEM image of the SiNPs@carbon nanofiber; (b) voltage profiles of the SiNPs@carbon nanofiber fabrics at 0.1 C rate and 0.01–1.5 V in half cells (the capacity vs. cycle number data was obtained at 0.1 C); and (c) plot of charge capacities vs. cycle number of the SiNPs@carbon nanofiber fabrics cycled (0.2 and 1 C) at 0.01–1.5 V and the pristine Si nanoparticles (0.1 C) [81]. Copyright 2013 Elsevier.

anodes can alleviate pulverization because nanosized Si is too small to break and a porous or hollow structure accommodates volume changes and carbon coating. In addition, a carbon coating creates a void that can accommodate volume changes and increase conductivity by enabling the formation of a direct contact space between the electrode and electrolyte [78, 79].

The Si/C nanofibers fabricated via electrospinning have several advantages: the fragile SEI formation on the surfaces of the Si nanoparticles can be avoided, and Si volume fluctuations during the insertion/extraction of Li ions can be mitigated by the carbon fibers [80, 81]. However, during the electrospinning process, nanosized Si aggregates and clusters are formed in the Si/C solution, impeding good dispersion within the nanofibers [82]. Researchers used a surfactant or a surface modification method to resolve this issue and obtain well-dispersed Si/C nanofibers [83]. Liu et al. [81] used 1 wt% SDBS as the surfactant during the electrospinning of Si/C nanofibers, achieving well-dispersed Si particles. As shown in Figure 17, the resultant fibers showed excellent cycling stability of 850 $mA{\cdot}hr{\cdot}g^{-1}$ over 100 cycles at 0.2 C and a rate capability of over 600 $mA{\cdot}hr{\cdot}g^{-1}$ at 1 C [81].

Xu et al.[84] monodispersed silicon nanoparticles in an aqueous solution via aminosilane functionalization with fluorine coordination (Figure 18). The treated Si nanoparticles bonded well with the polymer precursor and were completely encapsulated in amorphous carbon after carbonization,

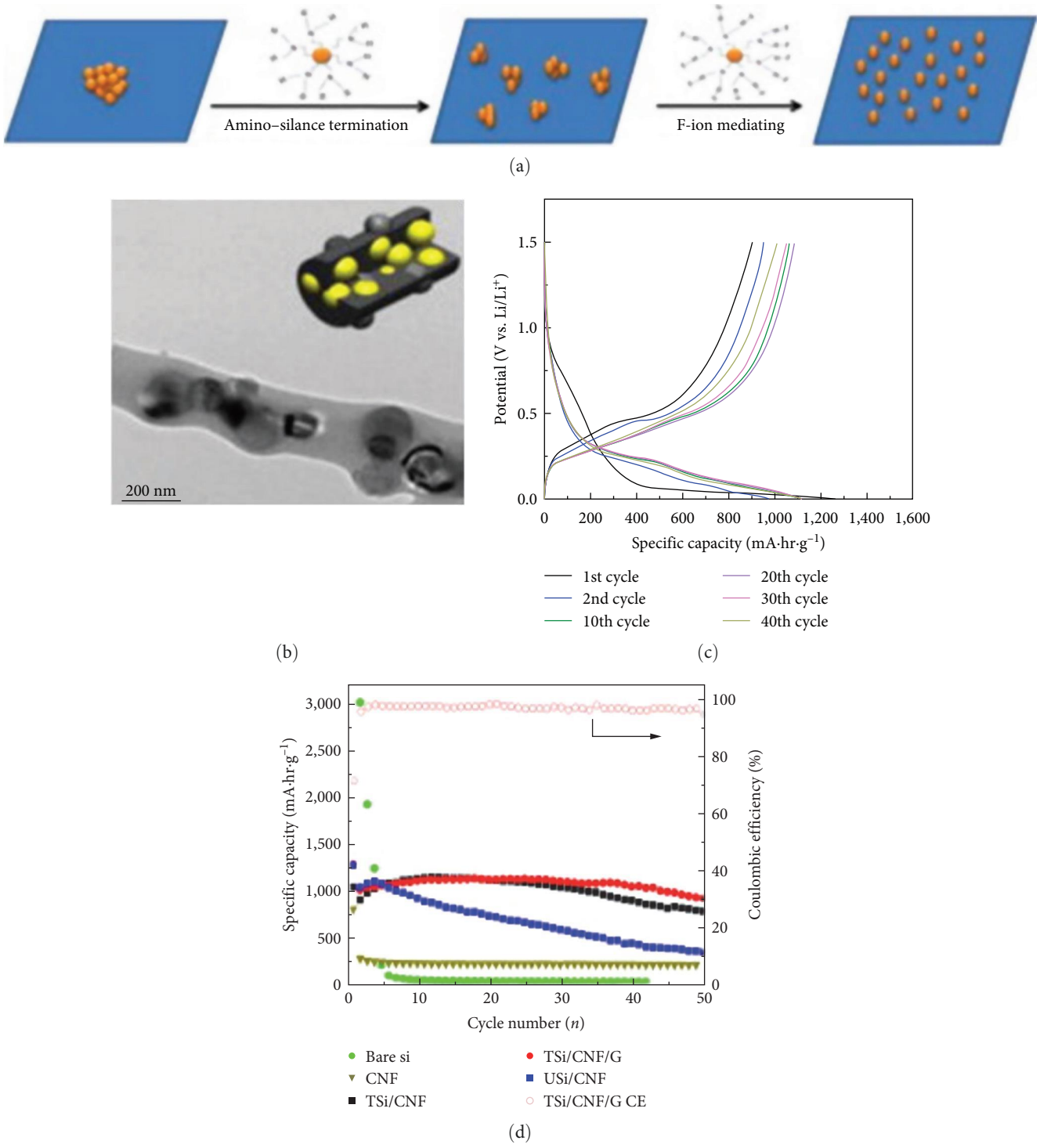

FIGURE 18: (a) Schematic diagram of amino–silane modification and F-ion mediation of Si nanoparticles; (b) corresponding HRTEM images and schematic; (c) charge/discharge voltage plot of TSi/CNF/G electrodes; and (d) rate performance of TSi/CNF and TSi/CNF/G electrodes measured at different rates of 100–1,000 mA·g^{-1} [84]. Copyright 2014 Elsevier.

serving as a stress buffer to mitigate the volume change caused by Si during cycling. As shown in Figures 18(c) and 18(d), the Si/carbon NF/graphite electrode exhibited 91% capacity retention with a discharge capacity of 872 mA·hr·g^{-1} after 50 cycles at 1.0 A·g^{-1} and a very good rate capacity of 567 mA·hr·g^{-1} [84].

5. Electrospun Nanofibers as Separator Materials

The separator is a porous film that prevents direct contact between the anode and cathode in an LIB and plays a role in the ionic flow. It also affects the internal resistance, which in

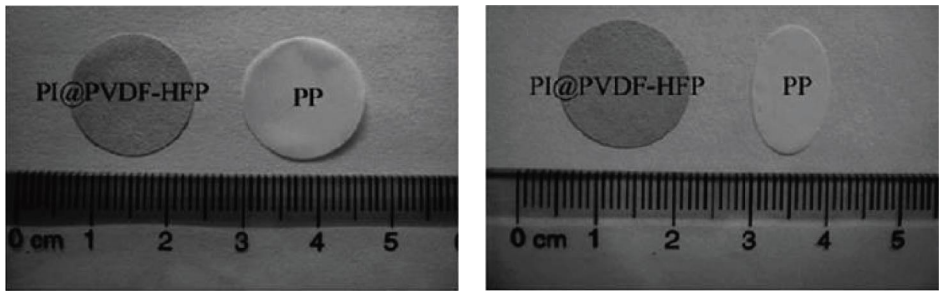

(a) (b)

FIGURE 19: Photographs of the polypropylene (PP) separator and nonwoven PI@PVDF–HFP (a) before and (b) after thermal treatment at 150°C for 1 hr [89]. Copyright 2013 Wiley.

turn affects the cycling and safety of the battery. Liquid electrolytes have traditionally been used to improve electrochemical performance. This is possible with high conductivity; however, it is highly likely to burn or explode, causing leakage. Therefore, despite their poor ionic conductivity, polymer- and ceramic-based materials are currently used because of battery safety issues. Currently, the most widely used separators in the LIB market are polyethylene (PE) and polypropylene (PP); however, they have weak electrolyte absorption capacity, low ionic conductivity, and poor thermal stability [85].

To improve the performance of LIB, the separator must have good mechanical strength, excellent thermal stability, high ion conductivity, and good wettability. A simple and inexpensive solution to these requirements is a 1-D electrospun fibrous-structure separator. Electrospun nanofibers have the advantages of a high surface area and porosity. In addition, nanofiber separators in LIBs exhibit high electrolyte absorption, substantial liquid retention, and excellent ionic conductivity [86]. Polymers such as polyvinylidene fluoride (PVDF), polyacrylonitrile (PAN), polyimide (PI), poly(m-phenylene isophthalamide) (PMIA), and polyvinylidene fluoride-co-hexafluoropropylene (PVDF-HFP) are subjected to electrospinning to fabricate nanofibers [87]. Among them, PVDF-HFP exhibits excellent electrochemical performance owing to its high affinity for a liquid electrolyte and can form a partial gel in an electrolyte. In addition, PVDF is generally used as an electrode binder in LIBs, and its copolymer binds well to electrodes and reduces interface resistance [88]. However, its only drawback is its low thermal stability. The PVDF-HFP nonwoven matrix shrinks with increasing temperature, which may cause stability problems in LIBs.

To overcome this issue, PI@PVDF-HFP core–shell structured fibers were fabricated via coaxial electrospinning. These fibers demonstrated a tensile strength of 53 MPa and high thermal stability at 300°C. In addition, they showed better rate capability and capacity retention than those of the existing separators by forming uniform and smaller pores [89]. Figure 19 shows the results for the effect of matrix shrinkage at high temperatures for conventional PP and PI@PVDf-HFP separators. After 1 hr of heat treatment at 150°C, it can be seen that PP has a very large thermal shrinkage, while the PI@PVDF-HFP separator with core–shell structure has no significant difference.

Bicomponent fibers, such as PVDF-HFP/PI, not only combine the strengths of PVDF-HFP and PI but also enhance and maintain them. The tensile strengths of PI and PVDF-HFP were 2.41 and 6.78 MPa, respectively, but that of PVDF-HFP/PI bicomponent fiber was 9.76 MPa, indicating enhanced mechanical properties. The physicochemical performance of the Celgard2030 membrane, which is often used as a separator in LIBs, was compared to that of the PVDF-HFP/PI separator. The contact angle was measured to show the difference in wettability and porosity. The contact angles of the nonwoven PVDF-HFP/PI were close to 0°, which suggests good wettability and affinity for electrolytes. In addition, its porosity was excellent, which led to improvements in ion conductivity and electrochemical performance. The most important issue when using polymer separators in LIBs is their thermal stability. The PVDF-HFP nanofibers shrank at high temperatures owing to their poor thermal stability. In Figure 20(a), While other separators shrink or deform during high-temperature heat treatment, the electrospun PVDF-HFP/PI bicomponent does not deform at high temperatures and has good thermal dimensional stability. Moreover, PVDF-HFP/PI showed a wider electrochemical stability window than that of Celgard2320. Its first discharge capacity was 120.41 $mA{\cdot}hr{\cdot}g^{-1}$ at 0.2 C, higher than the conventional Celgard separator and the coulombic efficiency was 99.36% (Figure 20(b)). After 50 cycles, the discharge capacity of Celgard2320 was maintained at 94.91%, whereas that of the PVDF-HFP/PI separator exhibited a higher retention performance of 98.13% (Figure 20(c)) [90].

The separator thickness of the LIB also has a profound effect on the electrochemical performance. The effect of separator thickness on electrochemical performance is briefly summarized in Table 1. Initially, the battery separator exhibited good performance while preventing contact between electrodes at the typical thickness of 25 μm [93]. Lim et al. [92], Choi et al. [91], and Costa et al. [87] studied the effect of electrospun PVDF nanofiber separator thickness on the electrochemical performance of the battery. Electrospun PVDF matrices are widely used as LIB membranes because they are very porous and can increase the pore size compared with other materials. In addition, the properties of PVDF, which is hydrophobic and piezoelectric, can be controlled by adding an appropriate nanofiller [92].

PVDF nanofiber separators exhibit higher porosity, desired fiber diameter, and optimal mechanical properties. However, if the membrane is too thick, the ionic conductivity decreases because the ion transport path becomes too long. Therefore,

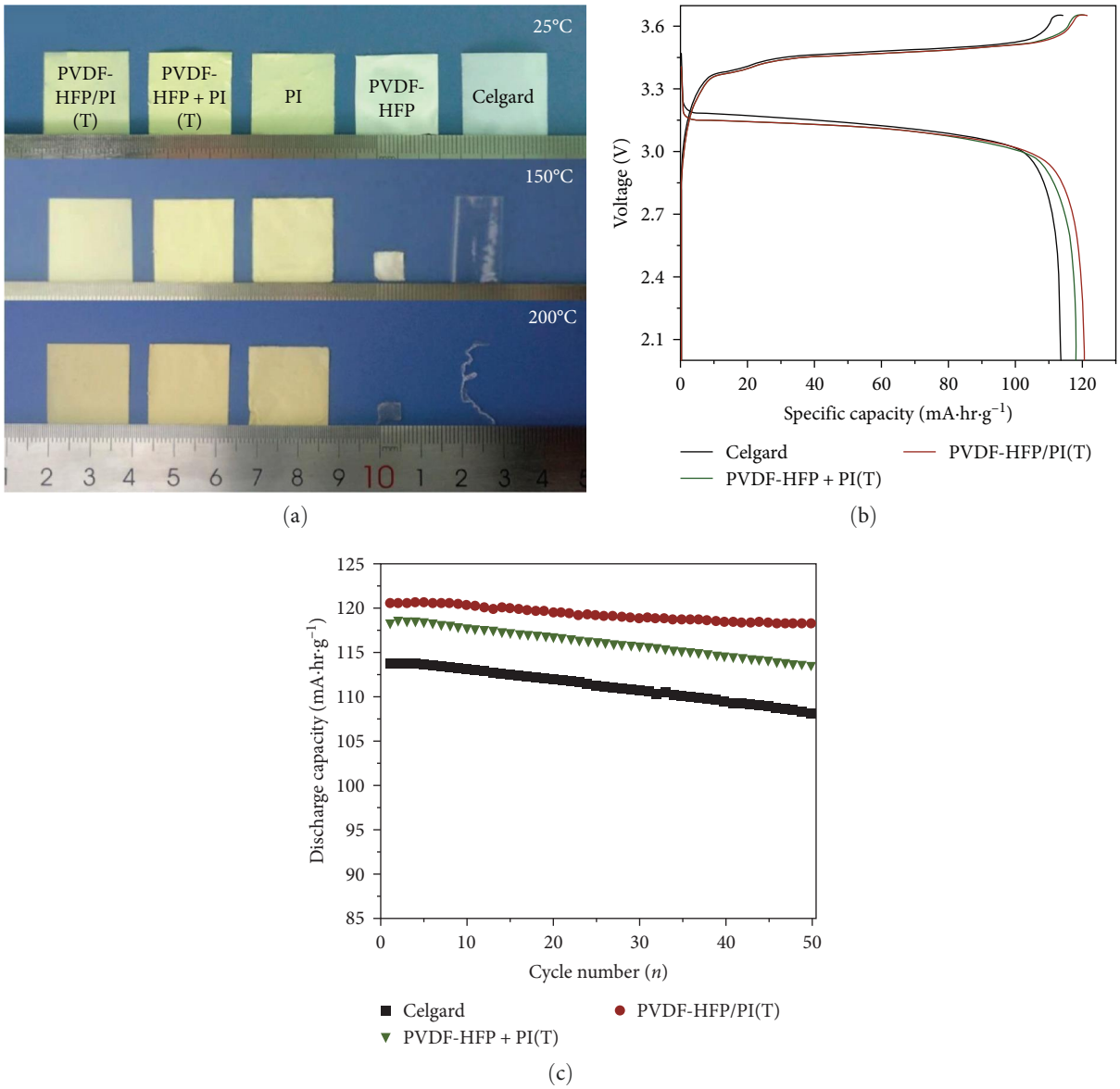

Figure 20: (a) Thermal dimensional stability of PVDF-HFP/PI electrospun membranes; (b) first charge/discharge curves; and (c) cycling performance of the Celgard2320 and PVDF-HFP/PI (T) separators at room temperature [90]. Copyright 2020 Elsevier.

Table 1: Comparison of the differences in ionic conductivity according to the thickness of electrospun PVDF nanofiber membranes.

Nanofiber separator	Fiber diameter (nm)	Membrane thickness (μm)	Ionic conductivity (S/cm)	Ref.
PVDF	100–800	20	$1.6–2.0 \times 10^{-3}$	[91]
PVDF	400	100	3.47×10^{-3}	[92]
PVDF	274 ± 96	160	4.0×10^{-6}	[87]

separator thickness has a significant impact on the electrochemical performance of LIBs.

6. Conclusion

The development of rechargeable batteries is very important owing to increasing energy demands. In particular, the development of LIBs, which exhibit high energy density, a long lifespan, and fast charging speed, is the most promising solution for meeting the exponentially increasing energy demands. However, LIBs may explode due to the formation of Li dendrites, experience capacity degradation, consume a high amount of resources, and cause environmental problems. The use of 1-D nanostructures prepared via electrospinning

emerged as a promising approach to improving the overall performance of LIBs.

Electrospinning technology is accessible and industrially scalable at a low price and enables precise control of the fiber morphology to afford flexible and other types of nanofibers. The mechanical strength of these nanofibers can be increased by optimizing the electrospinning parameters, while a hollow and porous nanostructure exhibits a high specific surface area. The use of this versatile electrospinning technique to prepare materials for LIB has resolved some of the physical and chemical problems of traditionally used bulk material electrodes. The use of these 1-D electrospun nanofibers as electrode materials in LIBs resulted in very short Li ion and electron diffusion paths and a large specific surface area for electrode/electrolyte interfaces, thereby increasing the charging/discharging capacity. Specific charges were increased, and the high surface-to-volume ratios further improved the performance by reducing the number of previously used Li particles. Issues such as the agglomeration of existing bulk materials have been resolved by incorporating composites to achieve the desired performance. Also, changing the structure through electrospinning allows for faster charging than traditional bulk cathodes. The use of these electrospun nanofibers can reduce costs while solving the volume expansion problem of existing LIB electrodes. Furthermore, these nanofibers enhanced the capacity retention and cyclic stability of the LIBs owing to their increased electrochemical performance.

The main advantage of applying electrospinning to LIBs is that the amount of material used can be reduced and the surface-to-volume ratio can be significantly increased through a 1-D structure. This increases the area for lithiation/delithiation of lithium during the charging/discharging process, thus improving the electrochemical performance of electrospun LIBs. In summary, the application of electrospinning technology to LIBs has the potential to increase the power density and energy density of batteries and to achieve high power and high energy density simultaneously. This promising technique can advance LIB technology to realize very-high-energy-density ESSs in the future.

Data Availability

The data that support the findings of this study are available on request from the corresponding author. The data are not publicly available due to privacy or ethical restrictions.

Conflicts of Interest

The authors declare that they have no conflicts of interest.

Acknowledgments

This work was supported by the Technology Innovation Program (or Industrial Strategic Technology Development Program-Public-private joint investment semiconductor R&D program (K-CHIPS) to foster high-quality human resources; RS-2023-00237003, High selectivity etching technology using cryoetch) funded by the Ministry of Trade, Industry & Energy (MOTIE, Korea) (1415187674). This work was also supported by the Technology Innovation Program (No. 20022472) funded by the Ministry of Trade, Industry and Energy (MOTIE, Korea). This research was also supported by the Basic Science Research Program through the National Research Foundation of Korea (NRF) funded by the Ministry of Education, Science and Technology (NRF-2022R1F1A1063561).

References

[1] F. Shi, C. Chen, and Z.-L. Xu, "Recent advances on electrospun nanofiber materials for post-lithium ion batteries," *Advanced Fiber Materials*, vol. 3, no. 5, pp. 275–301, 2021.

[2] M. Walter, M. V. Kovalenko, and K. V. Kravchyk, "Challenges and benefits of post-lithium-ion batteries," *New Journal of Chemistry*, vol. 44, no. 5, pp. 1677–1683, 2020.

[3] E. Fan, L. Li, Z. Wang et al., "Sustainable recycling technology for li-ion batteries and beyond: challenges and future prospects," *Chemical Reviews*, vol. 120, no. 14, pp. 7020–7063, 2020.

[4] J.-M. Tarascon and M. Armand, "Issues and challenges facing rechargeable lithium batteries," *Nature*, vol. 414, no. 6861, pp. 359–367, 2001.

[5] X. Zhang, L. Ji, O. Toprakci, Y. Liang, and M. Alcoutlabi, "Electrospun nanofiber-based anodes, cathodes, and separators for advanced lithium-ion batteries," *Polymer Reviews*, vol. 51, no. 3, pp. 239–264, 2011.

[6] A. K. Shukla and T. P. Kumar, "Nanostructured electrode materials for electrochemical energy storage and conversion," *WIREs Energy and Environment*, vol. 2, no. 1, pp. 14–30, 2013.

[7] D. H. Reneker and I. Chun, "Nanometre diameter fibres of polymer, produced by electrospinning," *Nanotechnology*, vol. 7, no. 3, pp. 216–223, 1996.

[8] S. Jayaraman, V. Aravindan, P. S. Kumar, W. C. Ling, S. Ramakrishna, and S. Madhavi, "Exceptional performance of TiNb2O7 anode in all one-dimensional architecture by electrospinning," *ACS Applied Materials & Interfaces*, vol. 6, no. 11, pp. 8660–8666, 2014.

[9] X. Li, Y. Chen, H. Huang, Y.-W. Mai, and L. Zhou, "Electrospun carbon-based nanostructured electrodes for advanced energy storage—a review," *Energy Storage Materials*, vol. 5, pp. 58–92, 2016.

[10] X. Yang, J. Wang, H. Guo, L. Liu, W. Xu, and G. Duan, "Structural design toward functional materials by electrospinning: a review," *e-Polymers*, vol. 20, no. 1, pp. 682–712, 2020.

[11] I. D. Norris, M. M. Shaker, F. K. Ko, and A. G. MacDiarmid, "Electrostatic fabrication of ultrafine conducting fibers: polyaniline/polyethylene oxide blends," *Synthetic Metals*, vol. 114, no. 2, pp. 109–114, 2000.

[12] G. R. Mitchell, *Electrospinning: Principles, Practice and Possibilities*, Royal Society of Chemistry, 2015.

[13] F. Mokhtari, M. Latifi, and M. Shamshirsaz, "Electrospinning/electrospray of polyvinylidene fluoride (PVDF) piezoelectric nanofibers," *Journal of the Textile Institute*, pp. 1–19, 2015.

[14] S. Haider, A. Haider, A. Ahmad, S. U.-D. Khan, W. A. Almasry, and M. Sarfarz, "Electrospun nanofibers affinity membranes for water hazards remediation," *Nanotechnology Research Journal*, vol. 8, no. 4, pp. 511–541, 2015.

[15] V. Pillay, C. Dott, Y. E. Choonara et al., "A review of the effect of processing variables on the fabrication of electrospun nanofibers for drug delivery applications," *Journal of Nanomaterials*, vol. 2013, pp. 1–22, 2013.

[16] B. Zaarour, W. Zhang, L. Zhu, X. Y. Jin, and C. Huang, "Maneuvering surface structures of polyvinylidene fluoride

nanofibers by controlling solvent systems and polymer concentration," *Textile Research Journal*, vol. 89, no. 12, pp. 2406–2422, 2019.

[17] L. Wannatong, A. Sirivat, and P. Supaphol, "Effects of solvents on electrospun polymeric fibers: preliminary study on polystyrene," *Polymer International*, vol. 53, no. 11, pp. 1851–1859, 2004.

[18] B. Zaarour, L. Zhu, C. Huang, and X. Jin, "Enhanced piezoelectric properties of randomly oriented and aligned electrospun PVDF fibers by regulating the surface morphology," *Journal of Applied Polymer Science*, vol. 136, no. 6, Article ID 47049, 2019.

[19] J. Fang, H. Niu, H. Wang, X. Wang, and T. Lin, "Enhanced mechanical energy harvesting using needleless electrospun poly(vinylidene fluoride) nanofibre webs," *Energy & Environmental Science*, vol. 6, no. 7, pp. 2196–2202, 2013.

[20] S. M. Damaraju, S. Wu, M. Jaffe, and T. L. Arinzeh, "Structural changes in pvdf fibers due to electrospinning and its effect on biological function," *Biomedical Materials*, vol. 8, no. 4, Article ID 045007, 2013.

[21] T. J. Sill and H. A. von Recum, "Electrospinning: applications in drug delivery and tissue engineering," *Biomaterials*, vol. 29, no. 13, pp. 1989–2006, 2008.

[22] H. Shao, J. Fang, H. Wang, and T. Lin, "Effect of electrospinning parameters and polymer concentrations on mechanical-to-electrical energy conversion of randomly-oriented electrospun poly(vinylidene fluoride) nanofiber mats," *RSC Advances*, vol. 5, no. 19, pp. 14345–14350, 2015.

[23] M. A. Zulfikar, I. Afrianingsih, M. Nasir, and A. Alni, "Effect of processing parameters on the morphology of pvdf electrospun nanofiber," *Journal of Physics: Conference Series*, vol. 987, Article ID 012011, 2018.

[24] A. S. Motamedi, H. Mirzadeh, F. Hajiesmaeilbaigi, S. Bagheri-Khoulenjani, and M. A. Shokrgozar, "Effect of electrospinning parameters on morphological properties of PVDF nanofibrous scaffolds," *Progress in Biomaterials*, vol. 6, no. 3, pp. 113–123, 2017.

[25] B. Kim, H. Park, S.-H. Lee, and W. M. Sigmund, "Poly(acrylic acid) nanofibers by electrospinning," *Materials Letters*, vol. 59, no. 7, pp. 829–832, 2005.

[26] S. De Vrieze, T. Van Camp, A. Nelvig, B. Hagström, P. Westbroek, and K. De Clerck, "The effect of temperature and humidity on electrospinning," *Journal of Materials Science*, vol. 44, no. 5, pp. 1357–1362, 2009.

[27] S. K. F. Ramakrishna, W. E. Teo, T.-C. Lim, and Z. Ma, *An Introduction to Electrospinning and Nanofibers*, World Scientific, 2005.

[28] B. Zaarour, L. Zhu, C. Huang, and X. Jin, "Controlling the secondary surface morphology of electrospun PVDF nanofibers by regulating the solvent and relative humidity," *Nanoscale Research Letters*, vol. 13, no. 1, pp. 1–11, 2018.

[29] J. I. Kim, J. C. Lee, M. J. Kim, C. H. Park, and C. S. Kim, "The impact of humidity on the generation and morphology of the 3D cotton-like nanofibrous piezoelectric scaffold via an electrospinning method," *Materials Letters*, vol. 236, pp. 510–513, 2019.

[30] B. Scrosati and J. Garche, "Lithium batteries: status, prospects and future," *Journal of Power Sources*, vol. 195, no. 9, pp. 2419–2430, 2010.

[31] A. O. Soge, A. A. Willoughby, O. F. Dairo, and O. O. Onatoyinbo, "Cathode materials for lithium-ion batteries: a brief review," *Journal of New Materials for Electrochemical Systems*, vol. 24, no. 4, pp. 229–246, 2021.

[32] J.-H. Shim, S. Lee, and S. S. Park, "Effects of MgO coating on the structural and electrochemical characteristics of $LiCoO_2$ as cathode materials for lithium ion battery," *Chemistry of Materials*, vol. 26, no. 8, pp. 2537–2543, 2014.

[33] S.-D. Zhang, M.-Y. Qi, S.-J. Guo et al., "Advancing to 4.6 V review and prospect in developing high-energy-density $LiCoO_2$ cathode for lithium-ion batteries," *Small Methods*, vol. 6, no. 5, Article ID 2200148, 2022.

[34] M. M. Thackeray, "Structural considerations of layered and spinel lithiated oxides for lithium ion batteries," *Journal of the Electrochemical Society*, vol. 142, no. 8, pp. 2558–2563, 1995.

[35] Y. Huang, Y. Dong, S. Li et al., "Lithium manganese spinel cathodes for lithium-ion batteries," *Advanced Energy Materials*, vol. 11, no. 2, Article ID 2000997, 2021.

[36] K. Ragavendran, H. Xia, P. Mandal, and A. K. Arof, "Jahn-teller effect in $LiMn_2O_4$: influence on charge ordering," *Physical Chemistry Chemical Physics*, vol. 19, no. 3, pp. 2073–2077, 2017.

[37] H. Zhou, X. Ding, Z. Yin et al., "Fabrication and electrochemical characteristics of electrospun $LiMn_2O_4$ nanofiber cathode for Li-ion batteries," *Materials Letters*, vol. 117, pp. 175–178, 2014.

[38] J. Liu, W. Liu, S. Ji, Y. Zhou, P. Hodgson, and Y. Li, "Electrospun spinel $LiNi_{0.5}Mn_{1.5}O_4$ hierarchical nanofibers as 5 v cathode materials for lithium-ion batteries," *ChemPlusChem*, vol. 78, no. 7, pp. 636–641, 2013.

[39] S. Patoux and M. M. Doeff, "Direct synthesis of $LiNi_{1/3}Co_{1/3}Mn_{1/3}O_2$ from nitrate precursors," *Electrochemistry Communications*, vol. 6, no. 8, pp. 767–772, 2004.

[40] Y. Zhou, C. Cao, F. Liu, D. Chen, and X. Jiao, "Core-shell Li$(Ni_{1/3}Co_{1/3}Mn_{1/3})O_2$/Li$(Ni_{1/2}Mn_{1/2})O_2$ fibers: synthesis characterization and electrochemical properties," *Solid State Ionics*, vol. 181, no. 15-16, pp. 678–683, 2010.

[41] C. Lv, J. Yang, Y. Peng et al., "1D Nb-doped $LiNi_{1/3}Co_{1/3}Mn_{1/3}O_2$ nanostructures as excellent cathodes for Li-ion battery," *Electrochimica Acta*, vol. 297, pp. 258–266, 2019.

[42] Y. Ding, P. Zhang, Z. Long, Y. Jiang, and F. Xu, "Morphology and electrochemical properties of Al doped $LiNi_{1/3}Co_{1/3}Mn_{1/3}O_2$ nanofibers prepared by electrospinning," *Journal of Alloys and Compounds*, vol. 487, no. 1-2, pp. 507–510, 2009.

[43] L. Tian, K. Liang, X. Wen, K. Shi, and J. Zheng, "Enhanced cycling stability and rate capability of $LiNi_{0.80}Co_{0.15}Al_{0.05}O_2$ cathode material by a facile coating method," *Journal of Electroanalytical Chemistry*, vol. 812, pp. 22–27, 2018.

[44] L. Zhang, Z. Zhao, X. Li et al., "Synthesis and electrochemical performance of ropelike $LiNi_{0.8}Co_{0.15}Al_{0.05}O_2$ fiber with nanobuilding blocks," *Materials Research Express*, vol. 7, no. 1, Article ID 015526, 2020.

[45] S. J. An, J. Li, C. Daniel, D. Mohanty, S. Nagpure, and D. L. Wood III, "The state of understanding of the lithium-ion-battery graphite solid electrolyte interphase (SEI) and its relationship to formation cycling," *Carbon*, vol. 105, pp. 52–76, 2016.

[46] C. Shen, G. Hu, L.-Z. Cheong, S. Huang, J.-G. Zhang, and D. Wang, "Direct observation of the growth of lithium dendrites on graphite anodes by operando EC-AFM," *Small Methods*, vol. 2, no. 2, Article ID 1700298, 2018.

[47] H. Zhang, Y. Yang, D. Ren, L. Wang, and X. He, "Graphite as anode materials: Fundamental mechanism, recent progress and advances," *Energy Storage Materials*, vol. 36, pp. 147–170, 2021.

[48] C. Kim, K.S. Yang, M. Kojima et al., "Fabrication of electrospinning-derived carbon nanofiber webs for the anode material of lithium-ion secondary batteries," *Advanced Functional Materials*, vol. 16, no. 18, pp. 2393–2397, 2006.

[49] B.-S. Lee, "A review of recent advancements in electrospun anode materials to improve rechargeable lithium battery performance," *Polymers*, vol. 12, no. 9, pp. 2035–2075, 2020.
[50] S. H. Senthilkumar, R. Brindha, R. P. Rao, V. Chellappan, and S. Ramakrishna, "Advances in electrospun materials and methods for li-ion batteries," *Polymers*, vol. 15, no. 7, pp. 1622–1652, 2023.
[51] S. N. Banitaba, D. Semnani, E. Heydari-Soureshjani, B. Rezaei, and A. A. Ensafi, "Electrospun core-shell nanofibers based on polyethylene oxide reinforced by multiwalled carbon nanotube and silicon dioxide nanofillers: a novel and effective solvent-free electrolyte for lithium ion batteries," *International Journal of Energy Research*, vol. 44, no. 8, pp. 7000–7014, 2020.
[52] M.-L. Hsiao and C.-T. Lo, "Hierarchical nanostructured electrospun carbon fiber/$NiCo_2O_4$ composites as binder-free anodes for lithium-ion batteries," *International Journal of Energy Research*, vol. 44, no. 11, pp. 8606–8621, 2020.
[53] J. Asenbauer, T. Eisenmann, M. Kuenzel, A. Kazzazi, Z. Chen, and D. Bresser, "The success story of graphite as a lithium-ion anode material—fundamentals, remaining challenges, and recent developments including silicon (oxide) composites," *Sustainable Energy & Fuels*, vol. 4, no. 11, pp. 5387–5416, 2020.
[54] Y. Chen, Z. Lu, L. Zhou, Y.-W. Mai, and H. Huang, "In situ formation of hollow graphitic carbon nanospheres in electrospun amorphous carbon nanofibers for high-performance Li-based batteries," *Nanoscale*, vol. 4, no. 21, Article ID 6800, 2012.
[55] Y. Chen, X. Li, K. Park et al., "Hollow carbon-nanotube/carbon-nanofiber hybrid anodes for Li-Ion batteries," *Journal of the American Chemical Society*, vol. 135, no. 44, pp. 16280–16283, 2013.
[56] S. W. Choi, J. R. Kim, S. M. Jo, W. S. Lee, and Y.-R. Kim, "Electrochemical and spectroscopic properties of electrospun pan-based fibrous polymer electrolytes," *Journal of the Electrochemical Society*, vol. 152, no. 5, Article ID A989, 2005.
[57] J. Jin, Z.-Q. Shi, and C.-Y. Wang, "Electrochemical performance of electrospun carbon nanofibers as free-standing and binder-free anodes for sodium-ion and lithium-ion batteries," *Electrochimica Acta*, vol. 141, pp. 302–310, 2014.
[58] S. Zhu, J. Sun, T. Wu et al., "Graphitized porous carbon nanofibers prepared by electrospinning as anode materials for lithium ion batteries," *RSC Advances*, vol. 6, no. 86, pp. 83185–83195, 2016.
[59] D. Wang, Z. Wang, Y. Li et al., "In situ double-template fabrication of boron-doped 3D hierarchical porous carbon network as anode materials for Li- and Na-ion batteries," *Applied Surface Science*, vol. 464, pp. 422–428, 2019.
[60] F. Tong, J. Guo, Y. Pan et al., "Coaxial spinning fabricated high nitrogen-doped porous carbon walnut anchored on carbon fibers as anodic material with boosted lithium storage performance," *Journal of Colloid and Interface Science*, vol. 586, pp. 371–380, 2021.
[61] D. Narsimulu, B. N. Rao, N. Satyanarayana, and E. S. Srinadhu, "High capacity electrospun $MgFe_2O_4$-C composite nanofibers as an anode material for lithium ion batteries," *ChemistrySelect*, vol. 3, no. 27, pp. 8010–8017, 2018.
[62] F. Pantò, Y. Fan, P. Frontera et al., "Are electrospun carbon/metal oxide composite fibers relevant electrode materials for Li-ion batteries?" *Journal of The Electrochemical Society*, vol. 163, no. 14, pp. A2930–A2937, A2930, 2016.
[63] J. Ling, C. Karuppiah, S. Das et al., "Quasi-anisotropic benefits in electrospun nickel-cobalt-manganese oxide nano-octahedron as anode for lithium-ion batteries," *New Journal of Chemistry*, vol. 46, no. 20, pp. 9799–9810, 2022.
[64] X. Qin, H. Zhang, J. Wu et al., "Fe_3O_4 nanoparticles encapsulated in electrospun porous carbon fibers with a compact shell as high-performance anode for lithium ion batteries," *Carbon*, vol. 87, pp. 347–356, 2015.
[65] L. Zhu, F. Li, T. Yao et al., "Electrospun $MnCo_2O_4$ nanotubes as high-performance anode materials for lithium-ion batteries," *Energy & Fuels*, vol. 34, no. 9, pp. 11574–11580, 2020.
[66] J. Wang, S. Xie, L. Li et al., "Electrospinning synthesis of porous NiCoO2 nanofibers as high-performance anode for lithium-ion batteries," *Particle & Particle Systems Characterization*, vol. 36, no. 7, Article ID 1900109, 2019.
[67] J. R. Szczech and S. Jin, "Nanostructured silicon for high capacity lithium battery anodes," *Energy & Environmental Science*, vol. 4, no. 1, pp. 56–72, 2011.
[68] B.-S. Lee, J. Yoon, C. Jung et al., "Silicon/carbon nanotube/$BaTiO_3$ nanocomposite anode: evidence for enhanced lithium-ion mobility induced by the local piezoelectric potential," *ACS Nano*, vol. 10, no. 2, pp. 2617–2627, 2016.
[69] S. Liang, X. Zhu, P. Lian, W. Yang, and H. Wang, "Superior cycle performance of sn@c/graphene nanocomposite as an anode material for lithium-ion batteries," *Journal of Solid State Chemistry*, vol. 184, no. 6, pp. 1400–1404, 2011.
[70] A. Mukhtar, S. S. Shafqat, M. N. Zafar, S. R. Shafqat, M. H.-U.-R. Mahmood, and S. Bashir, "3D nitrogen-doped graphene foam with encapsulated germanium/nitrogen-doped graphene yolk-shell nanoarchitecture for high-performance flexible Li-ion battery," *Nature Communications*, vol. 8, no. 1, pp. 1–9, 2017.
[71] R. Mo, D. Rooney, and K. Sun, "Yolk-shell germanium@polypyrrole architecture with precision expansion void control for lithium ion batteries," *Iscience*, vol. 9, pp. 521–531, 2018.
[72] A. R. Kamali and D. J. Fray, "Tin-based materials as advanced anode materials for lithium ion batteries: a review," *Reviews on Advanced Materials Science*, vol. 27, no. 1, pp. 14–24, 2011.
[73] J. Hassoun, G. Derrien, S. Panero, and B. Scrosati, "The role of the morphology in the response of Sb–C nanocomposite electrodes in lithium cells," *Journal of Power Sources*, vol. 183, no. 1, pp. 339–343, 2008.
[74] Q. Sun, Z. Cao, Z. Ma et al., "Dipole–dipole interaction induced electrolyte interfacial model to stabilize antimony anode for high-safety lithium-ion batteries," *ACS Energy Letters*, vol. 7, no. 10, pp. 3545–3556, 2022.
[75] Y. Zhao, J. Yan, J. Yu, and B. Ding, "Electrospun nanofiber electrodes for lithium-ion batteries," *Macromolecular Rapid Communications*, vol. 44, no. 4, Article ID 2200740, 2023.
[76] H. Wu and Y. Cui, "Designing nanostructured Si anodes for high energy lithium ion batteries," *Nano Today*, vol. 7, no. 5, pp. 414–429, 2012.
[77] B. Zhu, X. Wang, P. Yao, J. Li, and J. Zhu, "Towards high energy density lithium battery anodes: silicon and lithium," *Chemical Science*, vol. 10, no. 30, pp. 7132–7148, 2019.
[78] Y. Li, G. Xu, Y. Yao et al., "Coaxial electrospun Si/C-C core-shell composite nanofibers as binder-free anodes for lithium-ion batteries," *Solid State Ionics*, vol. 258, pp. 67–73, 2014.
[79] W. Lu, X. Guo, Y. Luo, Q. Li, R. Zhu, and H. Pang, "Core-shell materials for advanced batteries," *Chemical Engineering Journal*, vol. 355, pp. 208–237, 2019.
[80] Y. S. Kim, K. W. Kim, D. Cho, N. S. Hansen, J. Lee, and Y. L. Joo, "Silicon-rich carbon hybrid nanofibers from water-based spinning: the synergy between silicon and carbon for Li-ion battery anode application," *ChemElectroChem*, vol. 1, no. 1, pp. 220–226, 2014.

[81] Y. Liu, K. Huang, Y. Fan et al., "Binder-free Si nanoparticles@carbon nanofiber fabric as energy storage material," *Electrochimica Acta*, vol. 102, pp. 246–251, 2013.
[82] Y. Cui, "Silicon anodes," *Nature Energy*, vol. 6, no. 10, pp. 995-996, 2021.
[83] G. Hu, X. Zhang, X. Liu, J. Yu, and B. Ding, "Strategies in precursors and post treatments to strengthen carbon nanofibers," *Advanced Fiber Materials*, vol. 2, no. 2, pp. 46–63, 2020.
[84] Z.-L. Xu, B. Zhang, and J.-K. Kim, "Electrospun carbon nanofiber anodes containing monodispersed si nanoparticles and graphene oxide with exceptional high rate capacities," *Nano Energy*, vol. 6, pp. 27–35, 2014.
[85] J.-W. Jung, C.-L. Lee, S. Yu, and I.-D. Kim, "Electrospun nanofibers as a platform for advanced secondary batteries: a comprehensive review," *Journal of Materials Chemistry A*, vol. 4, no. 3, pp. 703–750, 2016.
[86] K. Bicy, A. B. Gueye, D. Rouxel, N. Kalarikkal, and S. Thomas, "Lithium-ion battery separators based on electrospun PVDF: a review," *Surfaces and Interfaces*, vol. 31, Article ID 101977, 2022.
[87] C. M. Costa, J. Nunes-Pereira, V. Sencadas, M. M. Silva, and S. Lanceros-Méndez, "Effect of fiber orientation in gelled poly (vinylidene fluoride) electrospun membranes for Li-ion battery applications," *Journal of Materials Science*, vol. 48, no. 19, pp. 6833–6840, 2013.
[88] H. Lee, M. Yanilmaz, O. Toprakci, K. Fu, and X. Zhang, "A review of recent developments in membrane separators for rechargeable lithium-ion batteries," *Energy & Environmental Science*, vol. 7, no. 12, pp. 3857–3886, 2014.
[89] Z. Liu, W. Jiang, Q. Kong et al., "A core@sheath nanofibrous separator for lithium ion batteries obtained by coaxial electrospinning," *Macromolecular Materials and Engineering*, vol. 298, no. 7, pp. 806–813, 2013.
[90] M. Cai, D. Yuan, X. Zhang et al., "Lithium ion battery separator with improved performance via side-by-side bicomponent electrospinning of PVDF-HFP/PI followed by 3D thermal crosslinking," *Journal of Power Sources*, vol. 461, Article ID 228123, 2020.
[91] S.-S. Choi, Y. S. Lee, C. W. Joo, S. G. Lee, J. K. Park, and K.-S. Han, "Electrospun PVDF nanofiber web as polymer electrolyte or separator," *Electrochimica Acta*, vol. 50, no. 2-3, pp. 339–343, 2004.
[92] S.-G. Lim, H.-D. Jo, C. Kim, H.-T. Kim, and D.-R. Chang, "Electro-spun poly(vinylidene fluoride) nanofiber web as separator for lithium ion batteries: effect of pore structure and thickness," *Journal of Nanoscience and Nanotechnology*, vol. 16, no. 1, pp. 956–961, 2016.
[93] Z. J. Zhang and P. Ramadass, "Lithium-ion battery systems and technology," in *Batteries for Sustainability: Selected Entries from the Encyclopedia of Sustainability Science and Technology*, pp. 319–357, Springer, New York, NY, 2012.